Final Report

PLUME RISE FROM KEYSTONE PLANT

by Betsy Woodard Proudfit
Sign X Laboratories, Inc.
Contract No. PH 86-68-94

203 767-1700

SIGN X LABORATORIES, INC.

ESSEX, CONNECTICUT 06426

Final Report

On

Plume Rise From Keystone Plant

Contract No. PH 86-68-94

15 March 1969
(Revised December 1970)

by

Betsy Woodward Proudfit

Prepared for: U. S. Department of Health, Education and Welfare
Public Health Service
Environmental Health Service
National Air Pollution Control Administration

CONTENTS

INTRODUCTION

A study to determine plume rise from a large power plant was undertaken by Sign X Laboratories, Inc., under contract from the U. S. Public Health Service.

The study was part of a larger research program conducted by the National Air Pollution Control Administration (NAPCA) to determine the extent and effects of power plant emissions from tall stacks.[1] Additional participants in the Large Power Plant Effluent Study (LAPPES) during the 1968 field experiments were Stanford Research Institute[2] and Meteorology Research Inc.[3]

The power plant studied was the Keystone Generating Station near Shelocta in western Pennsylvania. The station has a capacity of 1800 megawatts from two identical units. Each unit consists of one 244 meter stack and two 99-meter-tall natural draft cooling towers. During the May, 1968 field experiments Unit #1, only, was operating. Unit #2, only, was operating during the October, 1968 field studies.

The station is situated in a shallow valley. The surrounding terrain is hilly; the peaks of some of the hills within several kilometers of the site rise to about 100 m. above the stack base level (or about 150 m. below the top of the stack).

An instrumented helicopter was used to obtain a record of temperatures and sulfur dioxide concentration in the plume. The records were then evaluated to determine plume heights under a variety of atmospheric conditions. To assist in determining the plume boundaries, a device was used which detected charged particles in the plume. (At the request of NAPCA, about 50% of the electrostatic precipitators, which have an efficiency rating of 99.5%, were shut down during most of the observation periods.)

Data flights were made on seven days during May, 1968 and eight days during October, 1968. Data from ten days (two in May, eight in October) have been selected for inclusion in this report.

This report is composed of three parts. Part I describes the equipment and techniques used to obtain the data and the methods employed to reduce the data. Part II presents the data from ten flight days. Included are general descriptions of each day, temperature soundings and plume heights and SO_2 maximum concentrations obtained from traverses through the plume.

Part III presents an analysis and evaluation of twenty cases from seven flight days. For the cases analyzed, the average wind speed varied from 4.8 to 12.5 meters per second and the stability from about 0.15 to 1.5 degrees C. per 100 meters. This section, which is a paper that was presented at the North American Fuel Technology Conference, Ottawa, Canada, June, 1970, includes a summary of data acquisition and reduction in addition to an analysis of results.

References:

1. Schiermeier, F. A. and L. E. Niemeyer, 1970: Large Power Plant Effluent Study (LAPPES), Vol. 1 - Instrumentation, Procedures, and Data Tabulations (1968). National Air Pollution Control Administration Publication No. APTD 70-2.

2. Johnson, W. B., Jr. and E. E. Uthe, 1969: Lidar Study of Stack Plumes. Prepared for DHEW, NAPCA by Stanford Research Institute of Menlo Park, Calif., under contract No. PH 22-68-33.

3. Niemann, B. L., M. C. Day and P. B. McCready, Jr., 1970: Particulate Emissions, Plume Rise, and Diffusion from a Tall Stack. Prepared for DHEW, NAPCA by Meteorology Research, Inc. of Altadena, Calif., under contract No. CPA 22-69-20.

PART I - EQUIPMENT AND PROCEDURES

EQUIPMENT

The instrument package was flown in a 3-place (side by side) Bell 47 G helicopter which carried the pilot and the principal investigator, who acted as observer. The package, designed and fabricated by Sign X Laboratories, is similar to that used by PHS on the LAPPES Project and almost identical to that flown for the last several years by TVA.

Five variables, four at any one time, were recorded on two 2-pen, 10 inch, recorders. The variables were dry bulb temperature and SO_2 on one recorder and pressure height and wet-bulb depression or "space charge derivative" on the other.

1. Temperature: thermistor; time constant 0.1-0.2 seconds; 3 overlapping scales; 1°C = 0.5 inch.

2. SO_2: electroconductivity; time constant 2.0-2.5 seconds; 4 ranges, full scale (10 inches) 0-1.0, 0-2.5, 0-10, and 0-25 ppm.

3. Pressure height; double bourdon cell; electrical output linear function of pressure height according to standard atmosphere; time constant 0.1 sec.; 3 overlapping scales; 100 m = 1 inch.

4. Wet-bulb depression; 30 junction thermopile; time constant 0.1-0.2 sec.; 1 scale; 1°C = 0.5 inch.

5. Space charge; device measured change in space charge; not intended to be quantitative; instantaneous response.

There were two event markers on each recorder, one gave time marks every two minutes, the other was used for location, observations, etc. The chart speed was two inches per minute; the pen slewing speed 0.5 seconds for full scale deflection. The two pens, on each recorder, were overlapping so that both pens traversed the full 10-inch chart width. As a result the pens were off set a tenth of an inch (i.e. 3 seconds). This off set was taken into account during data reduction.

The two recorders were mounted in front of, and facing, the observer. The SO_2 unit and the inverter, for converting the helicopter's 24-volt DC power supply to 115 volts AC, were mounted on the seat between the pilot and the observer. The pressure height transducer was also mounted in the cockpit and was connected to the aircraft static line. The dry bulb temperature and wet bulb depression sensors were in a radiation housing mounted on the helicopter skid, well forward of the rotor downwash during normal operating speeds. The intake for the SO_2 analyzer and the space charge transducer were mounted next to the temperature housing.

The helicopter and instruments are shown in Figs. 1 and 2. Examples of the chart record are shown in Fig. 3.

FLIGHT PROCEDURES

The first flight of the day, during both the May and October series, commenced around dawn, weather permitting.

The equipment was turned on before take-off for a pre-flight check. During the flight from the airport to the Keystone site (about 15 min.) additional checks were made and meteorological conditions were noted.

The helicopter landed at the plant site and the aircraft's altimeter was set to 1000 feet (305 m.), the height of the stack base. The recorder pens for all four variables were moved simultaneously to establish the same time base for the two recorders and for pen off-set.

On many of the mornings ground fog obscured the plant site. The helicopter would then hover over the fog bank and, because warmer air would be brought down by the rotor, the fog would dissipate in the immediate area. This technique was successful except in one or two cases when the fog was exceptionally thick. (This technique, of dissipating fog, has been used by many helicopter pilots for a number of years.)

A temperature sounding was then made, just upwind of the stack, to a height of about 100 m. above the plume top, cloud cover permitting.

Two basic patterns were used to define the plume dimensions:

1. Slanting traverses. Starting from about 6 to 8 km. downwind a series of climbing and descending traverses were made through the plume, toward the stack. The track over the ground was generally fairly straight but the primary object was to traverse through the most dense part of the plume, rather than flying a straight course. The plume was often bifurcated, particularly within the first several kilometers of the stack. A chart of the area on which concentric circles, every kilometer, had been drawn, was used during the flights and position, usually every kilometer, was noted on the chart record by the event mark and in a notebook.

When a slanting traverse was made close to the stack, within 0.5 or 1.0 km., it was generally in the downwind direction, starting with a descending traverse from over the stack.

2. Horizontal traverses. This series of traverses was made across the plume at fixed distances, e.g. 4 km., downwind. A traverse was made just above the plume and was followed by traverses at 200 foot intervals until the base of the plume was reached. This was generally, but not always, followed by an ascending series, 100 feet, 300 feet, etc. higher until the plume top was reached. Thus a cross-section was obtained every 100 feet, or ~30 meters. Position was noted several times during each traverse.

Generally three series of slanting traverses, and two horizontal series, were flown during the first flight which lasted ~1.5 hours. Sometimes a constant level traverse, downwind, at the plume top was made. A second sounding was usually made during the latter part of the flight.

The second flight, about one hour later, lasted about two hours and was similar to the first. During the May session inversion breakup generally occurred prior to the second flight. During the October session it usually occurred near the end of the second flight. On some days a third flight was made.

Indicated air speed during all traverses and soundings was between 55 and 60 mph (~24 to 27 m/s).

DATA REDUCTION

Times (EST) and flight notes were transcribed on the chart records. The pressure height was traced onto the temperature and SO_2 chart record, to aid in reduction. Height and temperature were at the same time. SO_2, on the leading pen, was 3 seconds ahead.

Reduction of Pressure Height

The pressure height transducer, whose output is recorded on the chart, cannot be set to a particular height when the ambient pressure varies. It records absolute pressure, expressed in meters, according to the standard atmosphere. In order to obtain height above a surface, changes in ambient pressure must be taken into account.

The pressure heights at stack base level and at the airport were read from the chart records, at various times, for each flight day. These readings must be taken when the helicopter engine is off or at a low power setting. At full power, when on the ground or when hovering close to the ground, there is an increase in pressure of about one half millibar at the static position. This results in an indicated reading that is about 4 meters too low. The static is positioned so that correct readings may be obtained during normal flight speeds.

Graphs were made of pressure heights at stack base level vs time for each day. (Graphs for the October session are presented in Fig. 4) Also plotted on the graphs are pressure height at the airport minus 122 meters. (Height of airport: 427 m. ASL, stack base: 305 m. ASL). Pressure remained fairly constant on most days; on 22 Oct. a lowering of pressure gave a difference of 60 meters in 6.5 hours.

The value of the pressure height, H, shown on these graphs is then subtracted from the indicated readings in order to obtain height above stack base level, Z. No corrections have been made for the departure of the actual air temperature from the standard. The height, Z, should therefore be considered the pressure height above the stack base level. The difference between height, Z, and true height is small. The following computation gives an example.

On the morning of 20 October 1968 the surface temperature was about 12°C colder than standard (although at plume top level it was about 1°C warmer). If this temperature difference (i.e. the deviation from standard) is taken into account, then the true height of the plume top would be about 7 m. lower than the pressure height above stack base, Z.

The case above probably represents the greatest difference in height (between true height and pressure height, Z) of all the cases presented in this report. It would be reasonable to expect that the height error, due to a departure of the actual temperature from the standard, was less than 5 m. in the majority of cases. The probable pressure height error may be taken to be ± 10 m.

The heights that are given in the tables in Part II of this report are pressure heights above stack base level, Z. When potential temperature values were determined (see Analysis, Part III) the pressure height, H, was used.

Reduction of Dry Bulb Temperature

At air speeds above about 35 mph (~ 15 m/s) the temperature probe is in undisturbed air. Temperature readings taken when the aircraft is hovering close to the surface may be in error. "Surface" temperatures, for example those given in Part III, are therefore the temperatures measured 20 m. above the stack base level.

No correction has been made for the effect of dynamic heating. All soundings were made at an indicated air speed between about 24 and 27 m/s. The change in temperature due to a change in the air speed over this range is not greater than ± 0.1°C.

An absolute accuracy greater than ± 0.5°C is not claimed; however, it would be reasonable to expect that temperature measurements taken by the PHS helicopter and the Sign X helicopter would agree within a few tenths of 1.0°C. (The units were from the same manufacturer, the operational procedures were similar and a comparison flight was conducted.)

Reduction of SO_2 Data

All SO_2 values presented in this report are indicated readings.

The air sample (flow rate: 2500 cc/min.) and reagent (distilled water, flow rate: 25 cc/min.) are mixed. Any gas which changes the conductivity of the reagent will affect the accuracy of the SO_2 reading. However, the only gas which appears practically to cause a significant interference is CO_2. When determining low ambient SO_2 values it is necessary to measure the CO_2 background. This can be done by means of a scrubber, or bubbler, which selectively removes the SO_2. A series of calibration curves are then employed to determine the SO_2. For example, on the 1.0 ppm scale, the chart record would indicate 18% full scale for 0.2 ppm SO_2 and 0.0 ppm CO_2, 27% for 0.2 ppm SO_2 and 400 ppm CO_2, and 42% for 0.2 ppm SO_2 and 1000 ppm CO_2.

At higher SO_2 values the change in the indicated chart reading varies less with the change in CO_2. For example, on the 10.0 ppm scale when the SO_2 is 2.0 ppm, there is a 4% change in the full scale reading when the CO_2 varies from 0.0 to 2000 ppm.

During the plume rise studies described in this report it was not necessary to determine the ambient SO_2 and CO_2 values; therefore a bubbler was not used. The background, or ambient, readings recorded (and presented in Part II) are due to both SO_2 and CO_2.

In these studies, one is concerned with SO_2 values in the plume. There will of course be an increase in the CO_2 concentration in the plume. As the SO_2 value increases, the effect of changes in the CO_2 concentration decreases. For example, close to the stack, a concentration of 30 ppm SO_2 and 2100 ppm CO_2, above ambient, may be expected. At these high SO_2 values the indicated reading is the same whether the CO_2 is several hundred, or several thousand, ppm. Downwind, the SO_2 and CO_2 values will decrease and it is reasonable to assume they will decrease proportionally. For example, at a point downwind where the SO_2 concentration in the plume has decreased to 1.0 ppm, above ambient, then the CO_2 concentration will have decreased to 70 ppm, above ambient. On the 10. ppm scale, when the SO_2 concentration is 1.0 ppm, a 70 ppm change in CO_2 is equivalent to the width of the pen on the chart record.

For all practical purposes the effect of CO_2 interference, in these plume studies, may be neglected. The increase of SO_2 in the plume may be determined by simply subtracting the indicated background (ambient) reading.

The conductivity of the solution in the analytical cell of the SO_2 analyzer is temperature dependent. Compensation for temperature changes was not incorporated in the analyzer used in these studies. Sufficient tests have not been conducted to determine the degree of dependency.

At the start of each morning flight the reagent (distilled water) was comparatively cold. After the analyzer was turned on, the temperature of the reagent would increase due to heat generated by the recirculating pump. It would be reasonable to expect that the most rapid temperature changes (in the analytical cell) occurred shortly after start up. Approximately 25 minutes elapsed between start up and the first series of traverses. It would be reasonable to assume that the relative accuracy of the SO_2 values measured during the traverses on any one flight was about $\pm$ 10%.

It is, of course, not necessary to obtain absolute SO_2 values in order to determine plume rise. The above discussion has been made to facilitate understanding in case the SO_2 data presented in this report is used for other studies.

Reduction of Traverse Data

Horizontal Traverses: The maximum SO_2 value, recorded on each traverse, was read from the chart record and plotted vs. height. Examples of some of these plots are presented in Part II. Numerical values of SO_2 max. and height, for each series of horizontal traverses, are presented in tables in Part II. The indicated background SO_2 readings, obtained on the lowest and highest traverses, are also given.

Slanting Traverses: From the positions noted during a series of slanting traverses, a profile (height vs. distance downwind) was drawn. The heights of the plume top and bottom were determined from the SO_2 and "space charge" records and marked on the profile. The height and magnitude of the maximum SO_2 were also noted on the profile. Examples of some of these profiles, which also show a rough outline of the plume, are presented in Part II.

In addition to the 2 - 2 1/2 second time constant of the SO_2 analyzer, there is a delay time of 2 seconds. That is, it takes 2 seconds for the air sample to travel from the tube intake to the analytical cell. This delay does not distort the data; it simply offsets it by 2 seconds. When the plume was entered a delay time of 2 seconds was allowed; 3 seconds offset (equal to normal pen offset) was allowed when determining the height of the maximum SO_2. When the plume is left, a "tail-off" appears in the SO_2 trace. By comparing the SO_2 and space charge traces, it is possible, with a little practice, to take account of the "tail-off" effect.

The heights of plume top, bottom, and SO_2 maximum have been tabulated for various distances downwind and are presented in Part II. The heights, to the nearest 10 meters, and distances, to the nearest one tenth kilometer, that appear in the tabulations were read from the profiles.

Reduction of Wind Data

Wind speeds and directions were supplied by PHS personnel. A discussion is presented in Part III, Section 2. Graphs of wind speed and direction vs. time, for October 16, 20 and 22, 1968, are presented in Fig. 5.

Sign X Lab. Bell G2 Helicopter

Fig. 1

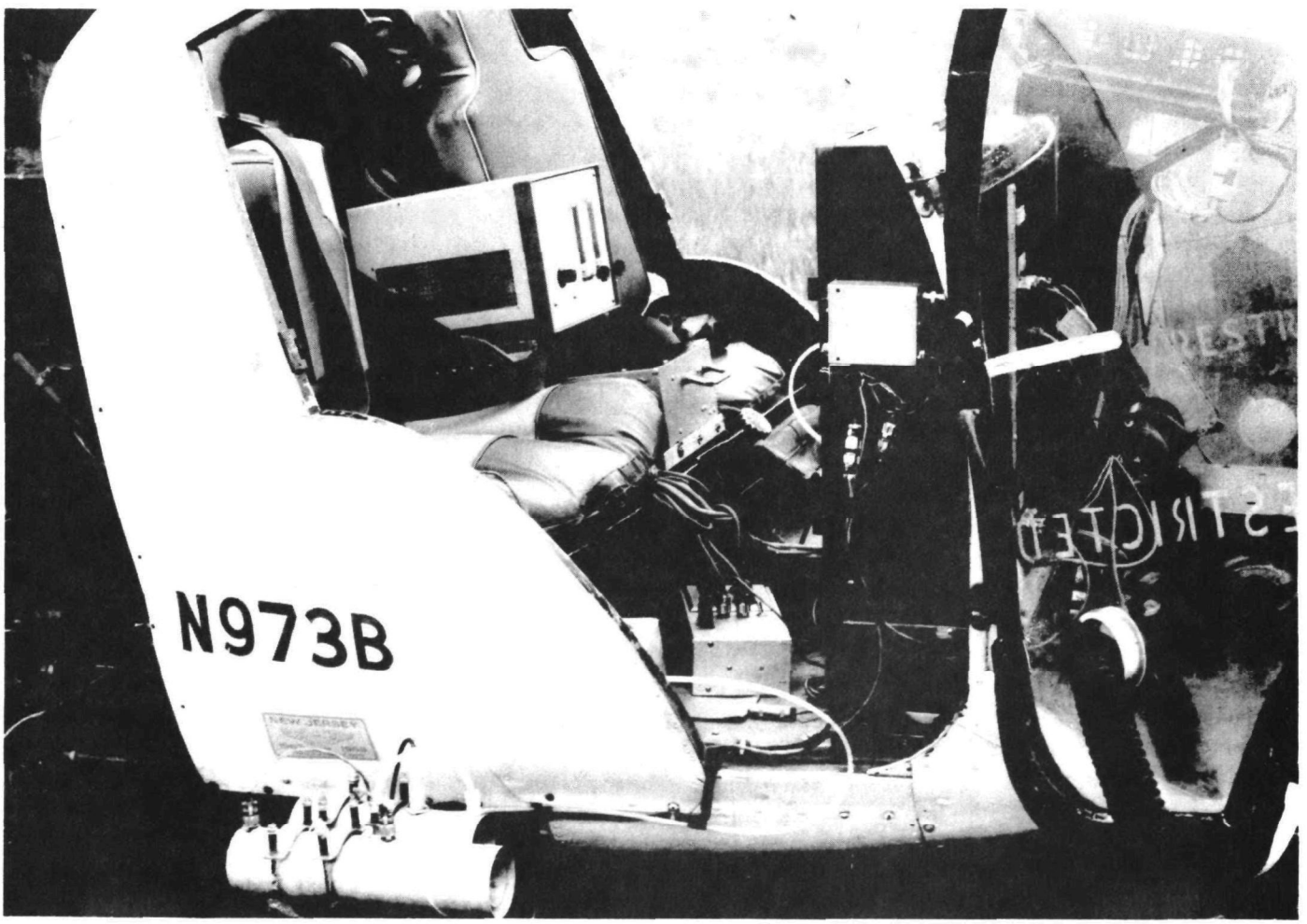

Sign X Lab. Model 6500B Package in G2, showing SO_2 Analyzer, DC-AC Inverter, and Power Distribution Box, and Dry Bulb Temperature, Wet Bulb Depression, and Space Charge Probes mounted on strut.

Fig. 2

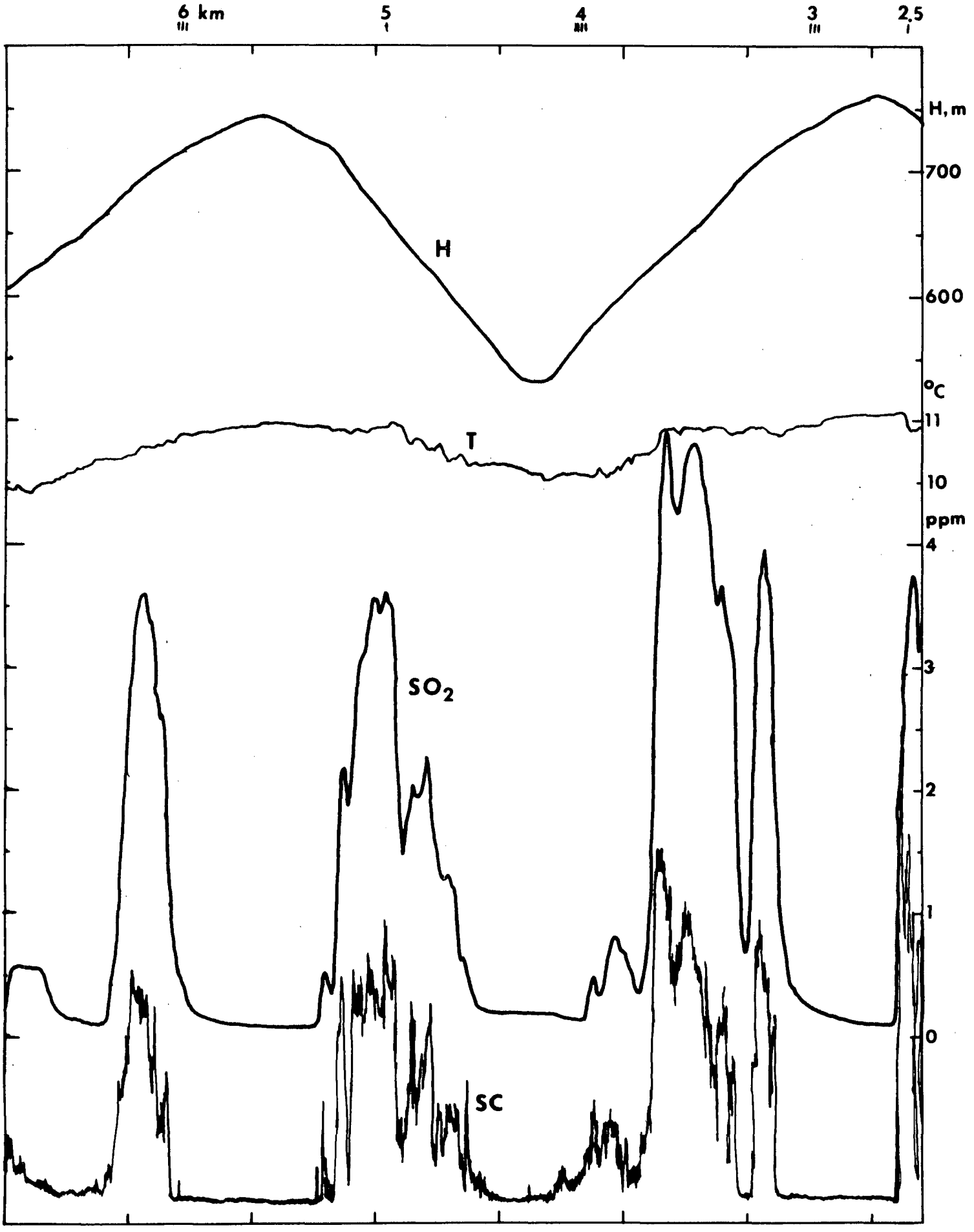

Fig. 3 Traces of pressure height, temperature, SO_2 and space charge derivative, from chart record between about 0707-0711 EST, 20 Oct. 68, during a series of slanting traverses from about 7 km downwind of the stack to 2.5 km.

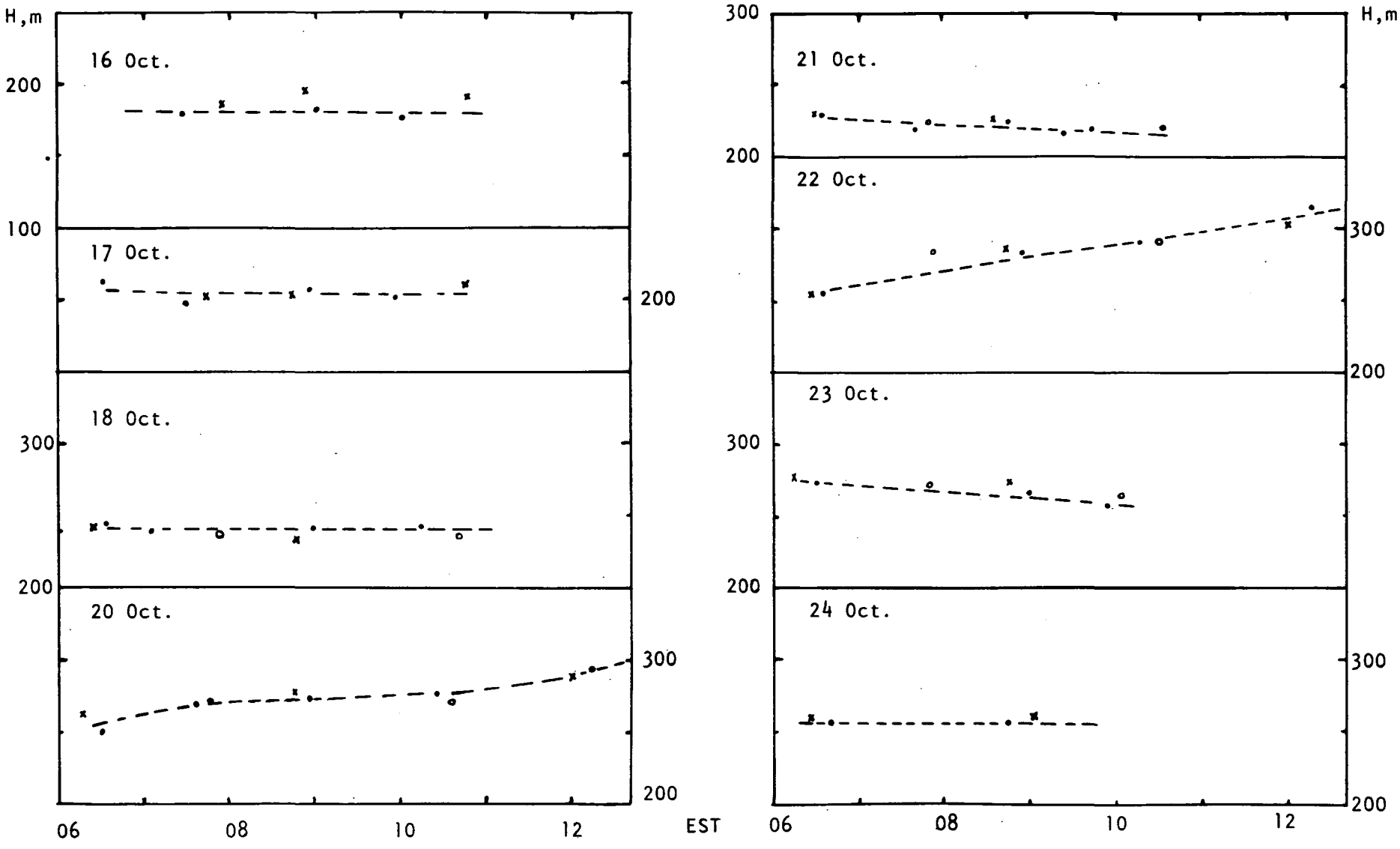

Fig.4. Solid dots indicate pressure height, H, at stack base level. Crosses and circles are pressure heights recorded at the airport, the difference in elevation having been taken into account. (Crosses: PHS landing area. Circles: gas pump area.)

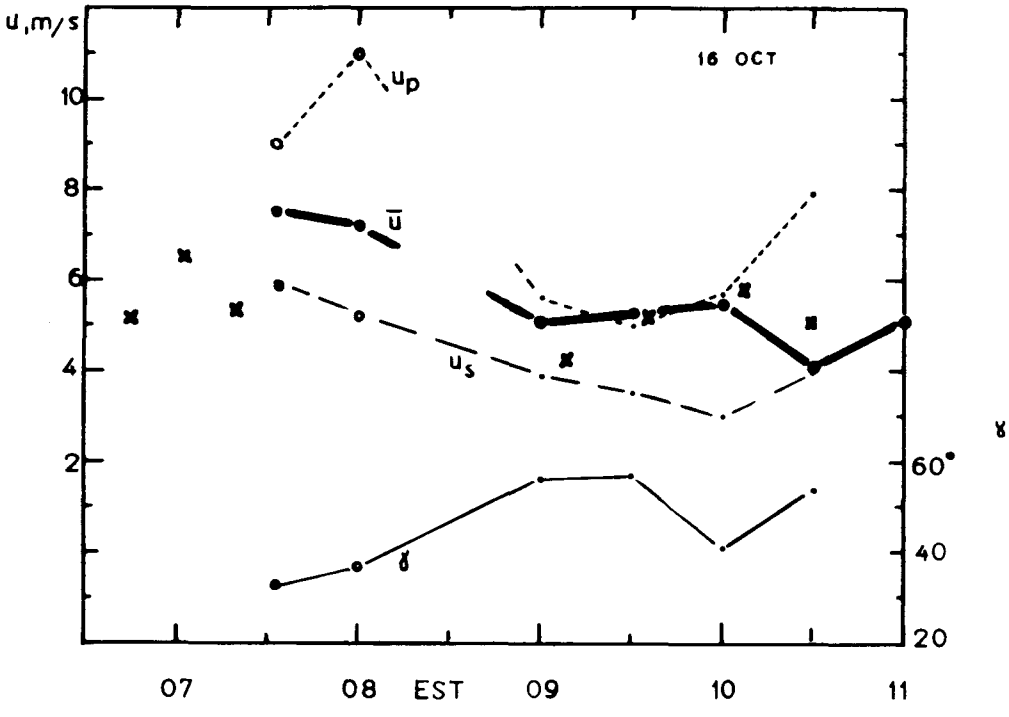

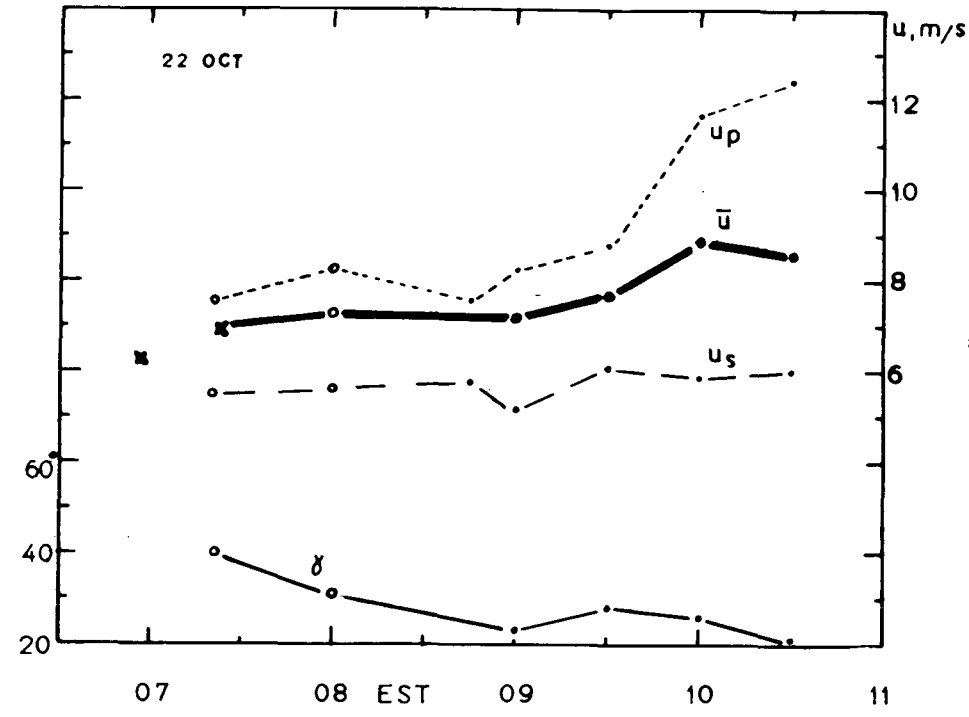

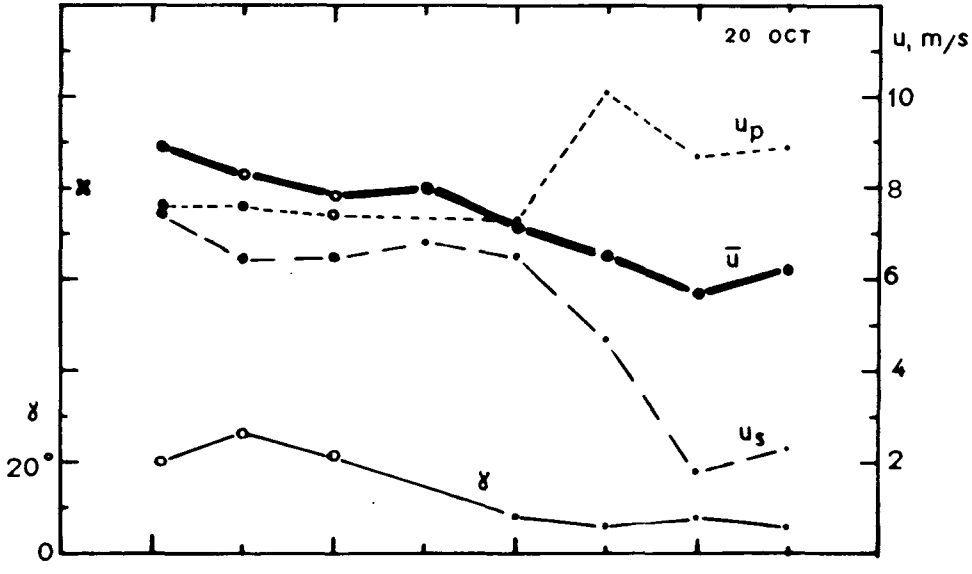

Fig. 5

o single theodolite measurements

●● double theodolite measurements

u_p Wind speed at plume top level (m/s)

u_s wind speed at stack top level (m/s)

$\bar{u}$ average wind speed between stack top and plume top, from pibals

x average wind speed computed from helicopter

γ directional shear (wind direction at plume top level minus wind direction at stack top level)

PART II - PRESENTATION OF DATA

PART II - PRESENTATION OF DATA

INTRODUCTION

Data from ten (of fifteen) flight days are presented in Part II. All data is included except that obtained when:

1. the plume was looping
2. the main plume and the cooling tower plume merged and remained saturated
3. the plume was in cloud

A short general description of all flight days is also presented.

The following data tabulations and diagrams are presented in Part II.

Tabulation of Traverse Data

For slanting traverses, the height, above stack base level, of the plume top, bottom and maximum SO_2 concentration and the value of the maximum concentration, are given for various distances downwind of the stack. Distances are to the nearest 0.1 km. and heights to the nearest 10 m.

For horizontal traverses, the value of the maximum SO_2 concentration obtained on each horizontal traverse through (and normal to) the plume is given for various heights above stack base level. The distance, X, from the stack, for each series of horizontal traverses, is noted. The indicated SO_2 reading obtained outside of plume (i.e. the background, or ambient reading) is given for the highest and lowest traverse in each series. The vertical arrows under the height column indicate the order in which the individual traverses were made. For example, on 17 Oct., page 36: the first traverse was made at 570 m. at 0643 EST. The subsequent traverses were made at descending levels to 270 m. The next traverse was at 420 m. and the last at 490 m. at 0655 EST.

The SO_2 values, in parts per million, are indicated readings (See p. 7). If a value is in parenthesis, it indicates that the recorder pen went off scale.

Temperature Sounding Diagrams

Plots of temperature soundings, made upwind of the stack, are presented. The temperature, in degrees centigrade, is shown vs. pressure height above stack base level.

Diagrams of Traverses

Some plots of horizontal and/or slanting traverses are presented. The diagrams of horizontal traverses show the maximum indicated SO_2 concentration encountered on each traverse, vs. pressure height above stack base level.

The dashed, or dotted, line in the plots of slanting traverses, indicate the path of the helicopter. The short bars represent plume top and bottom. On some of the plots the value of the maximum SO_2 concentration is given; on other plots the position where the maximum value was encountered is indicated by a circle. A rough outline of the plume is drawn.

Plots of Plume Heights and Potential Temperatures vs. Time

Plume heights (top, bottom, and height of SO_2 max.) and potential temperatures (at surface + 20 m., stack top, and plume top) were determined and plotted as a function of time for each day analyzed. Two of these plots, for 20 October and 22 October, appear in this section; a third, for 16 October, is shown in Part III.

The potential temperatures that are shown on these diagrams were obtained from soundings and also from additional readings obtained when in the vicinity of the stack (not in plume).

Additional Diagrams

Several diagrams, (e.g. Figs. 22-24) that have appeared in previous reports, are also included.

DAILY SUMMARIES

Note: The observations of cloud cover and precipitation, presented in the following short daily summaries, were made in the vicinity of the plant site, not at the Jimmy Stewart Airport.

22 May 1968

A short mid-day flight and an afternoon flight were made to check instruments, familiarize pilot and observer with terrain, and secondarily to obtain plume data. The stack precipitators were on so that the plume was not highly visible. During the first part of the afternoon flight there was a light drizzle to moderate rain; it then partially cleared. The plume was looping during part of the flight. No data is presented here.

23 May 1968

There was an overcast, light rain, and some fog in the valleys during a flight from 0745 to 0925. There was a ground based inversion to about 200 m. Above about 400 m., the lapse rate approached the dry adiabatic. The plume top, at about 3.0 km downwind, was at about 760 m., and plume thickness was about 300 m.

25 May 1968

Fog in the valleys prevented a sounding to ground level during the first flight. The sounding, from 0651 to 0658 EST was obtained when climbing downwind from the stack (adjacent to, but not in, the plume). The first flight was cut short to enable the lidar crew to make observations. During the third flight, from 1035 to 1235 EST, the temperature sounding was neutral. Winds were light; the plume was looping. Data from the first two flights are presented in this section.

26 May 1968

There was a 6/8 high overcast at the start of the first flight. The plume was fanning. At the start of the second flight, about 0900 EST, there was almost complete overcast. The plume was looping.

28 May 1968

There was complete overcast and a light drizzle. Visibility in the plume was zero, or nearly zero. During the first flight it was often impossible to fly above the plume; during the second it was never possible because of cloud base. The ceiling was less than 300 m. above stack top.

29 May 1968

There was early morning ground fog. Temperature soundings, at 0600 hrs. and 0830, were roughly isothermal. The cooling tower plume remained saturated and appeared to go higher than the main plume. There was merging of the two plumes.

31 May 1968

At 0600 hrs. the sounding showed a lapse rate similar to the moist adiabatic, with a shallow inversion at 400 m. There was a complete overcast. The cooling tower plume saturated the downwind region. The two plumes merged; the cooling tower plume went higher than the SO_2 plume. At 0745 hours a sounding was made. Temperatures approached the dry adiabatic rate; there was an inversion between 500 and 600 meters. The base of the lower cloud was at 350 m.

16 October 1968

There was early morning ground fog, especially in the vicinity of the plant. The plume was fanning. The second flight continued until inversion break-up, at about 1030 hours.

17 October 1968

There was light drizzle, with some intermittent light rain during the first flight. Cumulus formed at the top of the plume at 0930 hours during the second flight.

18 October 1968

There was again light drizzle with intermittent light rain. The drizzle continued during the second flight. There was some condensation in the plume at about 1000 hours.

20 October 1968

There was some early morning ground fog with clear skies above. During the second flight, at about 1000 hours, there was condensation intermittently at the plume top. There was indication that there was some merging of the cooling tower plume with the main plume. Also during the second flight the plume appeared (visually) to break into "rolls" or "waves" normal to the plume length.

21 October 1968

There was 4/8 high overcast at the start of the first flight. Later in the morning, around 1000 hours, clouds were forming in the plume.

22 October 1968

There was early morning ground fog. Plume "tilt", probably due to wind shear, was more apparent on this day than any other presented in this report. There were comparatively rapid changes, with time, of surface pressure and plant output. There was also an increase in the average wind speed during the second flight (0930-1000 hrs. EST). An appreciable wind increase occurred just above plume top level. This increase may have accounted for the apparent descent of the plume at about 0950. A third flight, made shortly after noon, showed adiabatic conditions. Horizontal traverses, at 3.4 km downwind, showed the plume extended above 850 m. and below 150 m.

23 October 1968

There were strong winds during the first flight. It was clear. There was some merging with the cooling tower plume but evaporation occurred within a few kilometers. Winds were lighter during the second flight. Some cumulus formed above, and in top of, the plume.

24 October 1968

A deep ground based inversion extended about 50 m. above the stack. Above this stable layer the lapse rate was close to neutral. The plume was lofting.

NOTATIONS - PART II

X Distance from stack, kilometers

Z Height above stack base level, meters

S ↑ Temperature sounding from stack base level to above plume top level (cloud permitting)

S ↓ Temperature sounding from above plume to stack base level (cloud permitting)

Traverses along X axis:

T ↖↙ Series of slanting traverses toward stack

T ↙↗ Series of slanting traverses away from stack

T ↘ Slanting traverse away from stack

T → Constant level traverse away from stack

Traverses normal to X axis:

T ⇄ Series of horizontal traverses across plume

Time is Eastern Standard.

TABULATIONS AND DIAGRAMS - PART II

Date: 25 May 68 Time: 0659-0704 Type Traverse: ↖✓

Distance Downwind	Height of Top	Height of Bottom	Max. SO_2	Max. SO_2
km	m	m	m	ppm
3.2	570			
3.0			490	3.7
2.8		450		
2.0		400		
1.8			470	2.5
1.7	530			
1.0	530			
0.9			450	3.6
0.8		410		

Date: 25 May 68 Time: 0854-0902 Type Traverse: ↖✓

5.5	610			
5.3			510	2.3
5.1		430		
4.9		410		
4.6			510	2.5
4.5	560			
3.7	560			
3.5			430	3.7
3.2		280		
2.6		310		
2.0	560		550	4.7
1.5	520			
1.4			490	5.0
1.2		400		
0.7		370		
0.6			410	15.5
0.4	490			

Date : 25 May 68 Time: 0920-24 Type Traverse: ↖✓

Distance Downwind	Height of Top	Height of Bottom	Height of Max. SO_2	Max. SO_2
km	m	m	m	ppm
1.7	650			
1.5			590	5.00
1.1		360		
0.5		310		
0.2			360	25.0
0.1	390			

Date: 25 May 68 Time: 0706-18 Type Traverse: ⇄

X = 1.2 km

Height, m ↓	Max. SO_2	Background SO_2
590	0.18	0.18
520	3.64	
440	(10.0+)	
390	6.98	
360	1.60	0.18

Date: 25 May 68 Time: 0903-19 Type Traverse: ⇄

X = 1.1 km

↓	↑		
	570	0.18	0.18
560		0.18	0.18
	540	8.23	
500		0.19	
	490	6.98	
430		8.64	
	420	1.82	
380		1.07	
350		0.76	0.19

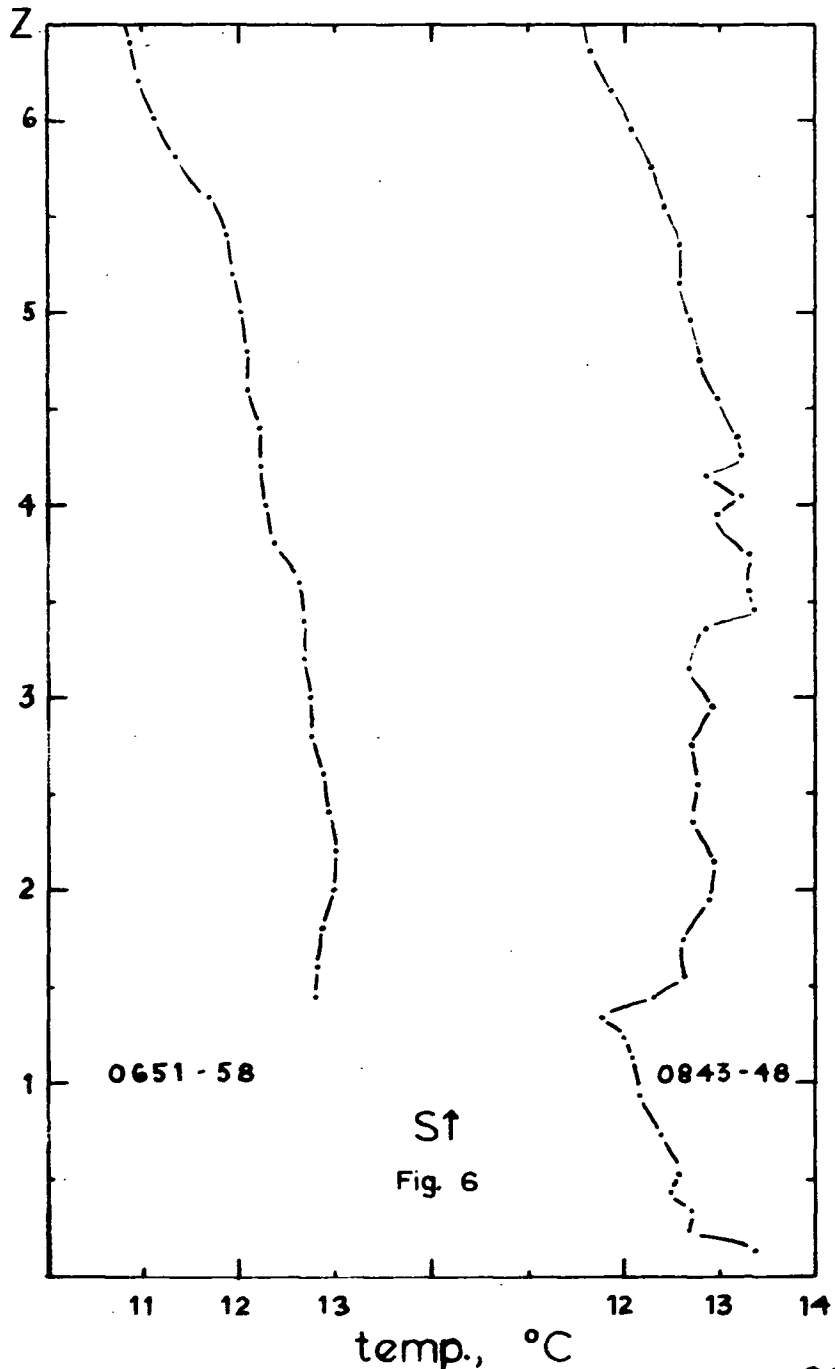
Z
6
5
4
3
2
1
0651 - 58
0843 - 48
S↑
Fig. 6
11
12
13
12
13
14
temp., °C

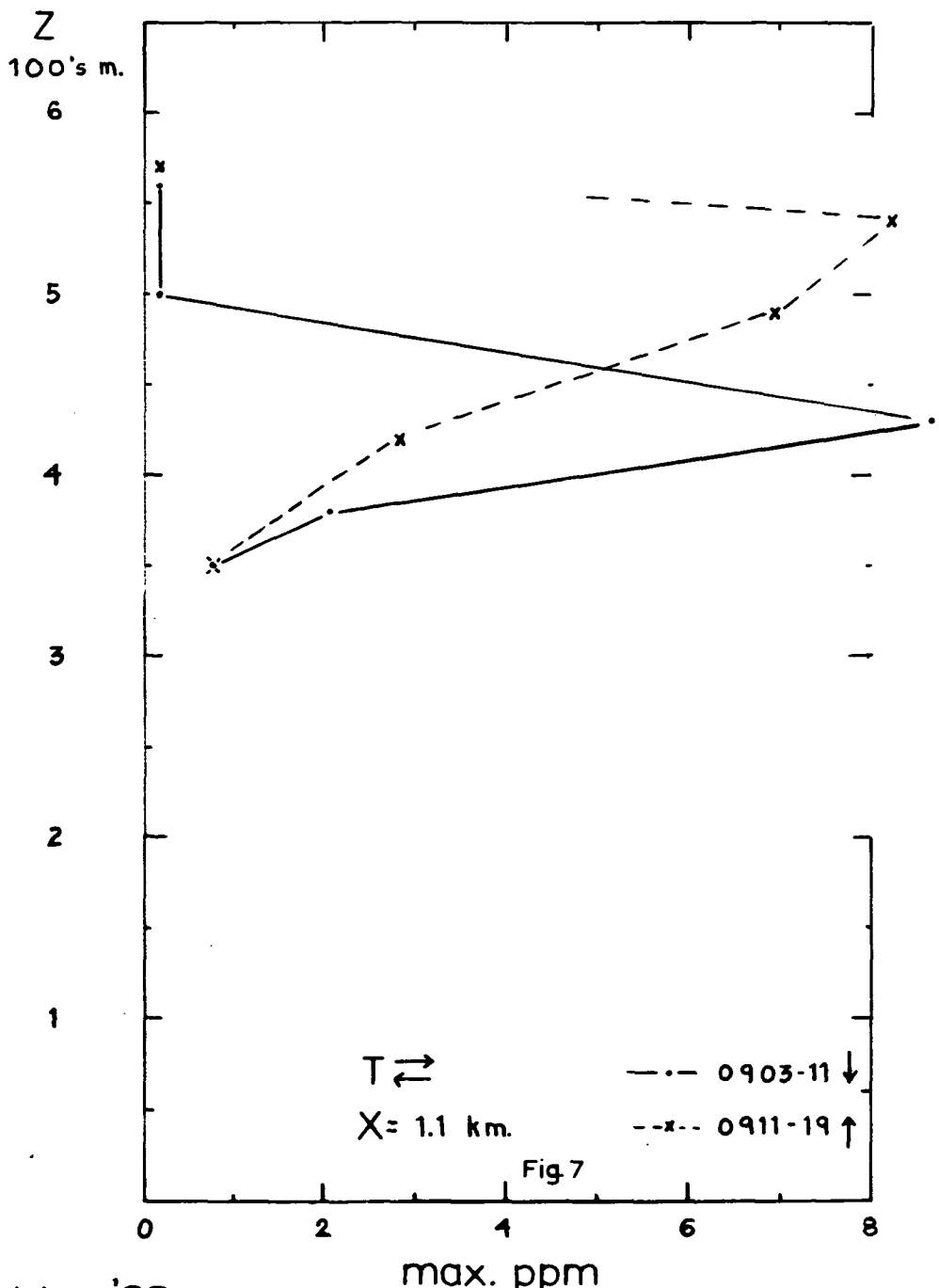
Z
100's m.
6
5
4
3
2
1
T ⇄
X= 1.1 km.
0903-11 ↓
0911-19 ↑
Fig. 7
0
2
4
6
8
max. ppm

25 May '68

24

Date: 26 May 68 Time: 0618-26 Type Traverse: ↖↙

Distance Downwind	Height of Top	Height of Bottom	Height of Max. SO_2	Max. SO_2
km	m	m	m	ppm
4.8	510			
4.6			400	1.25
4.5		370		
4.2		370		
4.0			420	1.35
3.9	460			
3.2	460			
3.0			410	1.50
2.8		370		
2.7		380		
2.5			450	2.90
2.4	470			
1.8	460			
1.6			390	6.50
1.4		340		
0.7	500			

Date: 26 May 68 Time: 0628-29 Type Traverse: ↘

0.2	410			
0.4			350	17.8
0.5		320		

Date: 26 May 68 Time: 0653-55 Type Traverse: ↖↙

1.8	510			
1.7			430	4.45
1.6		380		
1.4			430	(10.0+)
1.0	520			

Date: 26 May 68 Time: 0700-09 Type Traverse: ↖↙

4.0	550			
3.9			530	2.38
3.7		420		
3.5		390		
3.3			460	2.48
2.6	530			
2.5			460	4.00
2.2		370		
1.9			440	4.32
1.7	500			
1.4	530			
1.1			390	7.76
0.9		320		

Date: 26 May 68 Time: 0631-0650 Type Traverse: ⇄

X = 2.0 km

Height, m ↑	Height, m ↓	Max SO_2	Background SO_2
100		0.06	0.06
240		0.22	
280		4.92	
350		5.04	
	380	4.20	
420		5.33	
470		1.00	
	510	0.32	
550		0.06	0.06

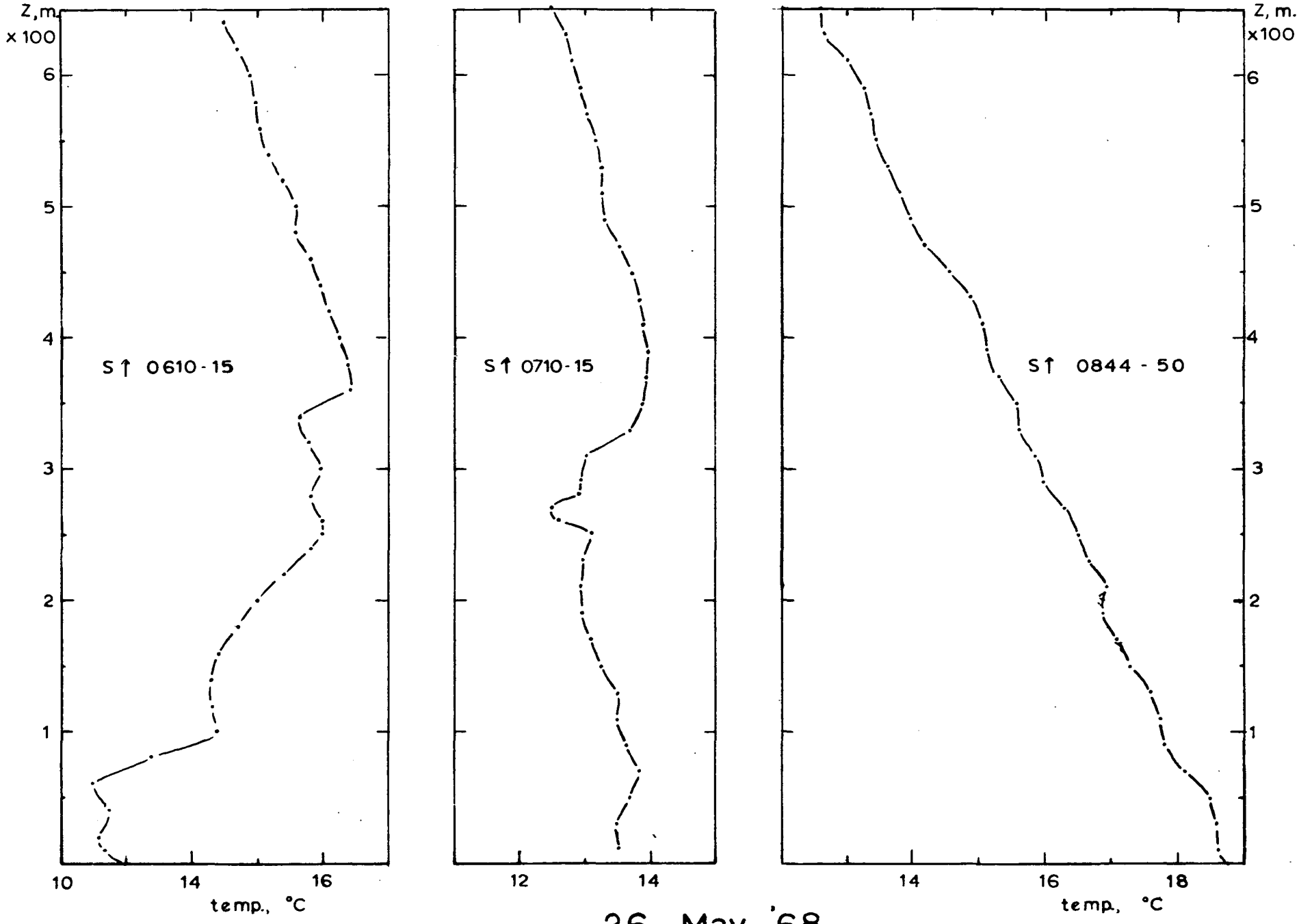

26 May '68

Fig. 8

Date: 16 Oct. 68 Time: 0659-0705 Type Traverse: ↖✓

Distance Downwind	Height of Top	Height of Bottom	Height of Max. SO_2	Max. SO_2
km	m	m	m	ppm
5.5	490			
5.3			420	4.61
5.1		370		
4.8		380		
4.7			420	4.72
4.5	460			
3.5	460			
3.3			400	5.20
3.1		330		
2.7		340		
2.3			400	6.68
1.8	510			
1.5	490			
1.2			400	(10.0+)
1.0		340		
0.8		350		
0.6			380	(25.0+)
0.2	440			

Date: 16 Oct. 68 Time: 0716-23 Type Traverse: ↖✓

7.5	540			
7.2			450	2.56
7.0		420		
6.8		420		
6.5			450	3.29
5.8	540			
5.7	540			
5.3			470	3.21
5.1		420		
4.9		420		
4.3			480	3.15
3.8	550			
3.5	540			
3.0			460	3.27
2.4		350		
2.0		340		
1.4			410	6.21
0.6	530			

Date: 16 Oct. 68 Time: 0738-42 Type Traverse: ↖↙

Distance Downwind	Height of Top	Height of Bottom	Height of Max. SO_2	Max. SO_2
km	m	m	m	ppm
4.6	480			
4.3			430	2.42
4.1		390		
3.7		390		
3.4			420	2.62
2.9	500			
2.3			450	3.25
2.1		380		
1.7		390		
1.4			430	7.84
1.0	520			

Date: 16 Oct. 68 Time: 0912-16 Type Traverse: ↖↙

5.7	540			
5.3			470	1.79
5.0		410		
3.5		410		
2.9			480	2.69
2.5	540			
1.7	550			
1.6			530	3.86
1.0		390		

Date: 16 Oct. 68 Time: 0918-19 Type Traverse: ↘

0.5	540			
0.8			500	7.98
2.0		340		

Date: 16 Oct. 68 Time: 0933-38 Type Traverse: ↖↘

Distance Downwind	Height of Top	Height of Bottom	Height of Max. SO_2	Max. SO_2
km	m	m	m	ppm
6.0	540			
5.8			500	2.29
5.6		450		
4.7		400		
4.0			490	3.11
3.6	540			
2.6	510			
2.4			480	2.00
2.1		380		
1.4		400		
0.7			500	4.41
0.5			550	4.96
0.3	570			

Date: 16 Oct. 68 Time: 1005-1011 Type Traverse: ↖↘

6.1	600			
6.0			560	0.83
5.9		530		
5.1		460		
4.2			560	1.17
3.9	610			
3.0	570			
2.9			540	1.13
2.7		450		
2.0		460		
1.1			620	2.9
0.8	650			

Date: 16 Oct. 68 Time: 1027-32 Type Traverse: ↖↘

6.6	700			
6.1			580	1.10
5.5		460		
4.4		480		
3.2			670	1.30
2.4			780	1.59
1.6			840	2.08
0.9			890	2.55
0.7	910			

Date: 16 Oct. 68 Time: 0650-56 Type Traverse ⇄

X = 2.9 km

Height, m ↓	Max. SO_2	Background SO_2
570	0.10	0.10
540	2.42	
500	2.70	
430	3.60	
370	1.10	
310	0.36	0.10

Date: 16 Oct. 68 Time: 0707-12 Type Traverse: ⇄

X = 2.0 km

↓		
560	0.13	0.13
490	2.57	
440	3.40	
370	2.20	
310	0.15	0.15

Date: 16 Oct. 68 Time: 0730-37 Type Traverse: ⇄

X = 2.9 km

↓		
510	0.10	0.10
480	0.10	
450	2.98	
380	1.80	
320	0.29	0.13

Date: 16 Oct. 68 Time: 0920-30 Type Traverse: ⇄

X = 2.9 km

Height, m ↑	Height, m ↓	Max. SO_2	Background SO_2
270		0.18	0.18
320		0.18	0.18
380		1.11	
450		2.72	
	490	3.23	
510		3.23	
	550	2.13	
580		1.18	
	600	0.19	
620		0.18	0.18

Date: 16 Oct. 68 Time: 0940-55 Type Traverse: ⇄

X = 2.0 km

Height, m ↓	Height, m ↑	Max. SO_2	Background SO_2
640		0.20	0.20
580		1.90	
	550	2.01	
	480	2.20	
450		2.40	
	420	2.09	
400		1.88	
	350	0.71	
320		0.52	
260		0.29	0.20

Date: 16 Oct. 68 Time: 1012-24 Type Traverse: ⇄

X = 3.0 km

Height, m ↓	Max. SO_2	Background SO_2
630	0.47	0.20
580	1.83	
530	1.13	
450	0.58	
390	0.71	
320	0.22	0.20

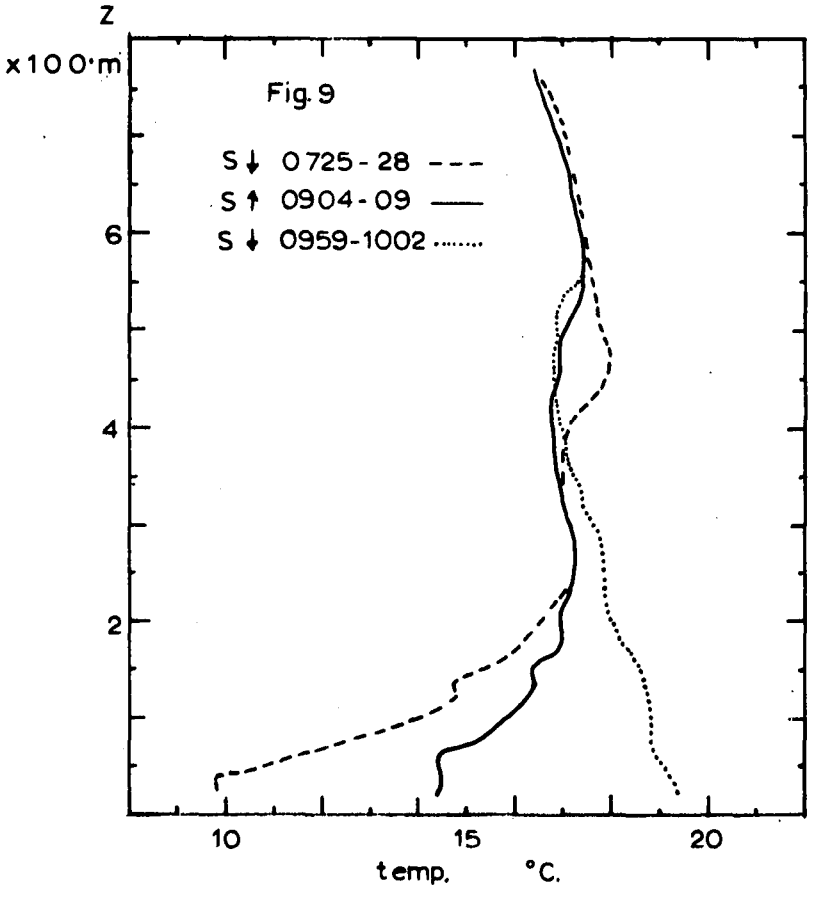
Z
x100·m
Fig. 9
S ↓ 0725-28 ---
S ↑ 0904-09 ——
S ↓ 0959-1002 .....
6
4
2
10
15
20
temp. °C.

16 Oct. '68

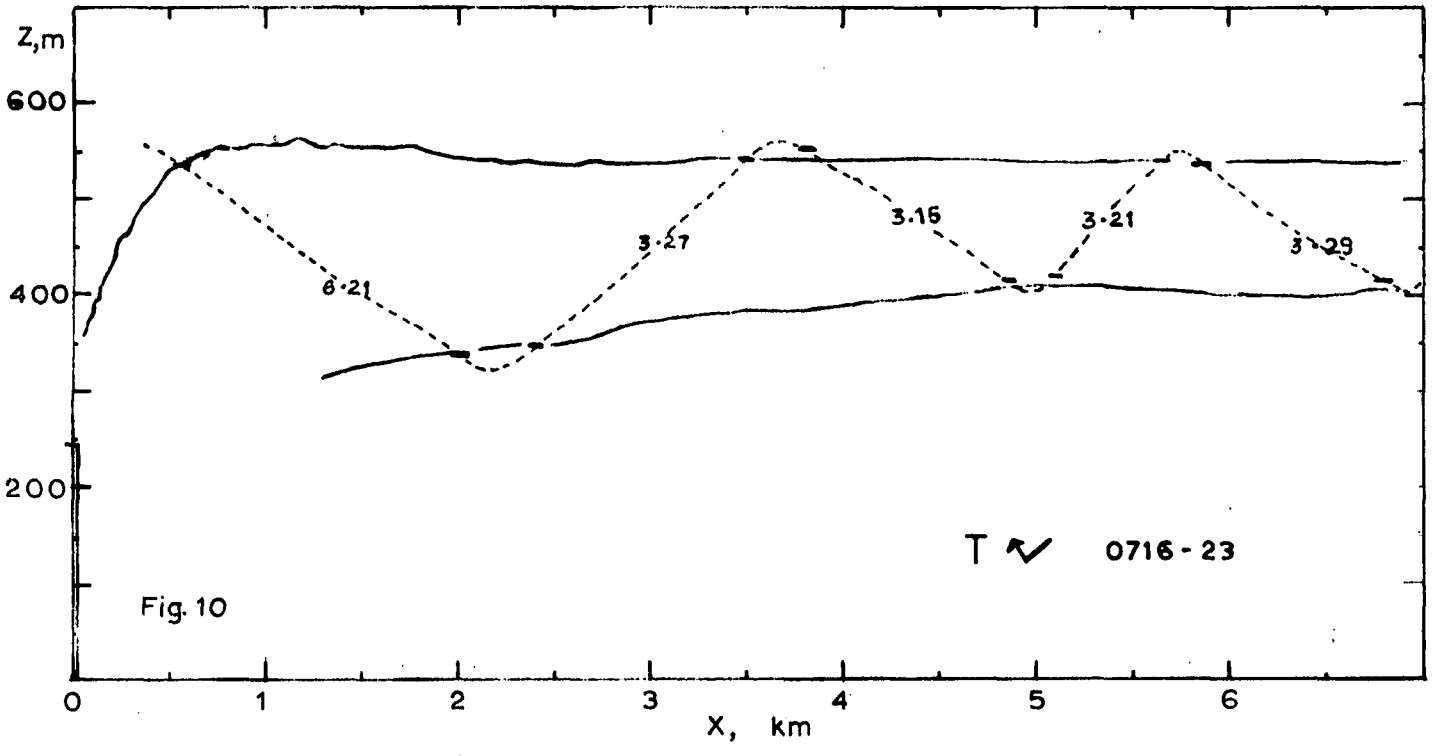
Z,m
600
400
200
6·21
3·27
3·15
3·21
3·29
T ~ 0716-23
Fig. 10
0
1
2
3
4
5
6
X, km

Date: 17 Oct. 68 Time: 0635-41 Type Traverse: ↖↙

Distance Downwind	Height of Top	Height of Bottom	Height of Max. SO_2	Max. SO_2
km	m	m	m	ppm
5.8	470			
5.6			420	0.46
5.3		350		
4.4		360		
3.9			450	(1.0+)
3.6			490	1.91
3.4	520			
2.6	510			
2.4			460	2.26
1.9		350		
1.8		340		
1.4			450	6.82
1.1	510			

Date: 17 Oct. 68 Time: 0658-0705 Type Traverse: ↖↙

5.0		360		
4.5			460	1.35
4.3	500			
3.5	500			
2.7		300		
2.3		300		
1.5			460	4.5
1.2	520			

Date: 17 Oct. 68 Time: 0705-07 Type Traverse: ↘

0.8	500			
1.1			480	7.30

Date: 17 Oct. 68 Time: 0722-29 Type Traverse: ↖✓

Distance Downwind	Height of Top	Height of Bottom	Height of Max. SO_2	Max. SO_2
km	m	m	m	ppm
6.6			480	0.90
6.3		390		
5.8		380		
5.4			460	1.23
4.9	560			
4.2	570			
4.1			540	2.21
3.5		380		
3.1		400		
2.5			520	5.17
2.3	560			
1.7	540			
1.4			430	6.45
1.1		360		

Date: 17 Oct. 68 Time: 0906-13 Type Traverse: ↖✓

9.0	660			
8.6			590	0.47
6.5		460		
6.0			530	0.87
5.2	660			
4.3	650			
3.7			510	0.98
3.0		410		
2.3			490	2.24
2.0	550			
1.5	580			
1.4			560	4.58

Date: 17 Oct. 68 Time: 0915-16 Type Traverse: ↘

0.9	510			
1.0			490	7.15
2.4		290		

Date: 17 Oct. 68 Time: 0643-55 Type Traverse: ⇄

X = 2.9 km

Height, m. ↓	Height, m. ↑	Max. SO_2	Background SO_2
570		0.09	0.08
520		1.80	
	490	2.33	
460		2.78	
	420	1.36	
380		0.87	
320		0.49	
270		0.09	0.09

Date: 17 Oct. 68 Time: 0708-19 Type Traverse: ⇄

X = 2.0 km

Height, m. ↑	Height, m. ↓	Max. SO_2	Background SO_2
210		0.10	0.10
310		0.69	
380		1.11	
	420	2.77	
450		3.58	
	470	3.38	
500		3.18	
	540	3.63	
570		0.89	
590		0.10	0.10

Date: 17 Oct. 68 Time: 0917-40 Type Traverse: ⇄

X = 3.0 km

Height, m. ↑	Height, m. ↓	Max. SO_2	Background SO_2
250		0.52	0.20
320		0.43	
380		0.43	
440		0.60	
	490	0.69	
520		0.91	
	540	2.00	
560		1.34	
	600	1.39	
630		1.46	
	650	2.37	
690		1.18	
	710	0.82	
770		0.18	0.18

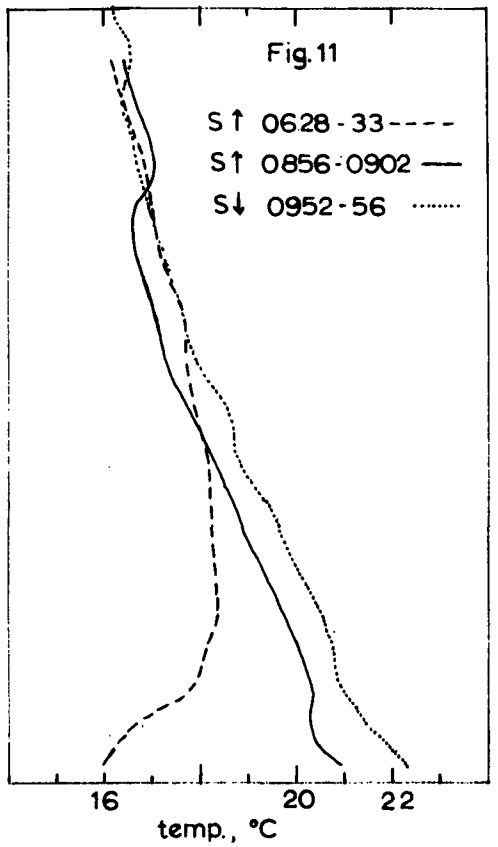
Fig.11
S↑ 0628-33
S↑ 0856-0902
S↓ 0952-56
16
20
22
temp., °C

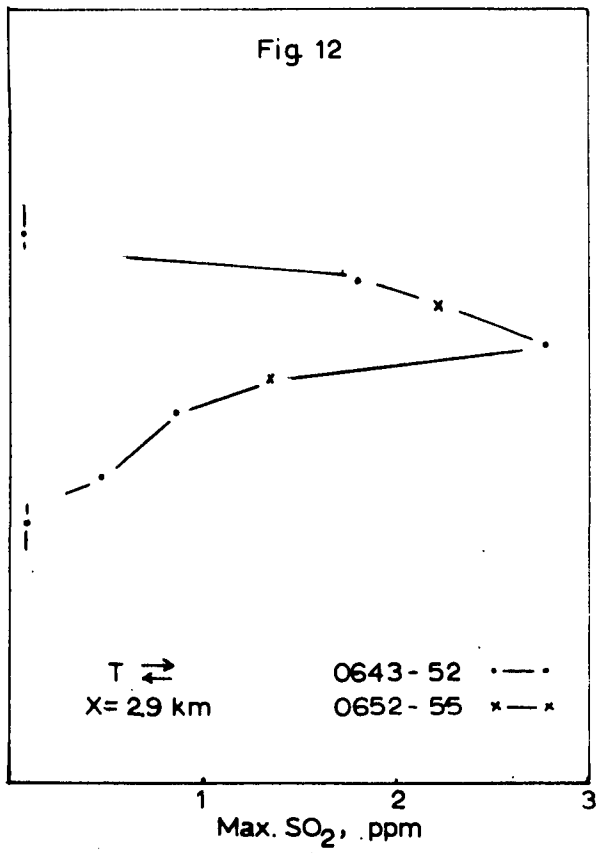
Z, m.
Fig. 12
600
400
200
T ⇄
X= 2.9 km
0643-52
0652-55
1
2
3
Max. SO2, ppm

17 Oct. '68

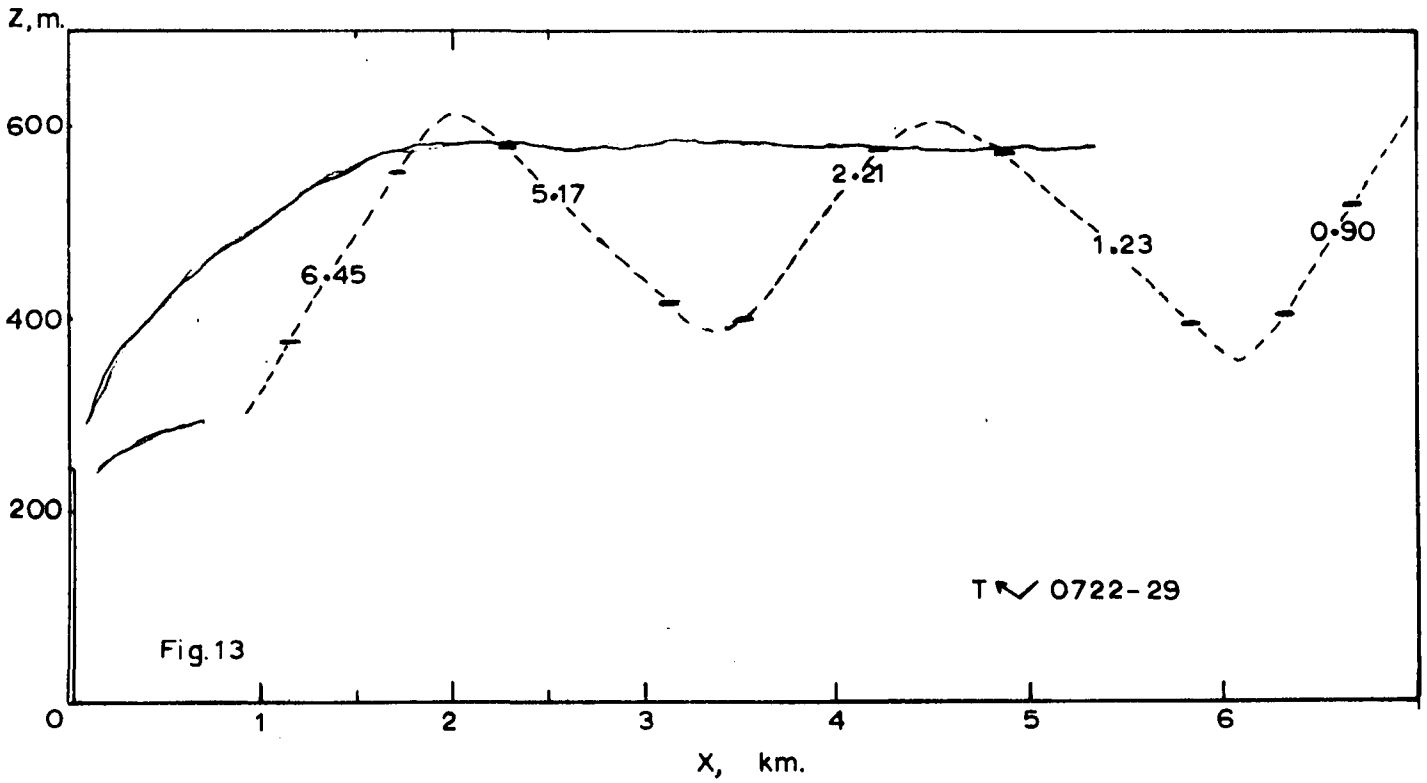
Z, m.
600
400
200
0
6.45
5.17
2.21
1.23
0.90
T ↘ 0722-29
Fig.13
1
2
3
4
5
6
X, km.

Date: 18 Oct. 68 Time: 0657-0701 Type Traverse: ↖↘

Distance Downwind	Height of Top	Height of Bottom	Height of Max. SO_2	Max. SO_2
km	m	m	m	ppm
5.0	620			
4.8			550	1.61
4.3		420		
3.9		430		
3.5			520	0.93
3.4	540			
2.9	600			
2.4			500	3.58
1.7		360		

Date: 18 Oct. 68 Time: 0708-15 Type Traverse: ↖↘

6.8			510	1.32
6.5		430		
6.0		450		
5.8			510	1.22
5.5	590			
5.1	600			
4.7			490	1.32
4.4		400		
3.9		430		
3.4			550	1.12
2.9	620			
2.5	580			
2.3			520	2.13
1.8		370		

Date: 18 Oct. 68 Time: 0717-19 Type Traverse: ↗↘

0.9	510			
1.2			480	5.01
2.6			510	2.73
3.7	640			

Date: 18 Oct. 68 Time: 0734-40 Type Traverse: ↖✓

Distance Downwind	Height of Top	Height of Bottom	Max. SO_2	Max. SO_2
km	m	m	m	ppm
6.2	630			
5.9			520	1.39
5.6		430		
5.3		430		
5.1			490	1.21
4.3			500	0.80
4.0		380		
3.6		350		
2.5	530			

Date: 18 Oct. 68 Time: 0907-13 Type Traverse: ↖✓

8.9	750			
7.7			460	0.85
7.2		360		
6.7		370		
5.5			550	0.60
5.3	580			
4.1	560			
3.7			480	0.94
2.8		310		
1.4			520	3.62
1.1	570			

Date: 18 Oct. 68 Time: 0914-16 Type Traverse: ↘

0.9	530			
1.1			490	6.36
2.2		300		

Date: 18 Oct. 68 Time: 0642-55 Type Traverse: ⇄

X = 3 km

Height, m ↑	Height, m ↓	Max. SO_2	Background SO_2
270		0.10	0.10
390		0.40	
460		1.62	
	490	1.99	
520		1.93	
	540	2.12	
570		2.13	
	610	2.50	
640		2.40	
	660	0.09	0.09
700		0.09	0.09

Date: 18 Oct. 68 Time: 0720-33 Type Traverse: ⇄

↓	↑	X = 4.0 km	
700		0.11	0.11
640		1.64	
	600	1.22	
560		2.26	
	540	2.77	
510		2.03	
	490	1.06	
450		1.02	
390		0.54	
320		0.20	0.12

Date: 18 Oct. 68 Time: 0920-34 Type Traverse ⇄

X = 5.7 km

Height, m ↑	Max. SO_2	Background SO_2
320	0.26	0.15
380	0.34	
460	0.61	
510	0.69	
570	0.96	
640	0.73	
700	0.54	
760	0.53	
820	0.14	0.14

Date: 18 Oct. 68 Time: 0948-1002 Type Traverse: ⇄

X = 3.9 km

↓		
940	0.15	0.15
880	0.63	
830	0.16	
760	0.99	
700	0.88	
640	1.11	
560	1.03	
510	0.90	
460	0.67	
380	0.60	
320	0.32	0.16

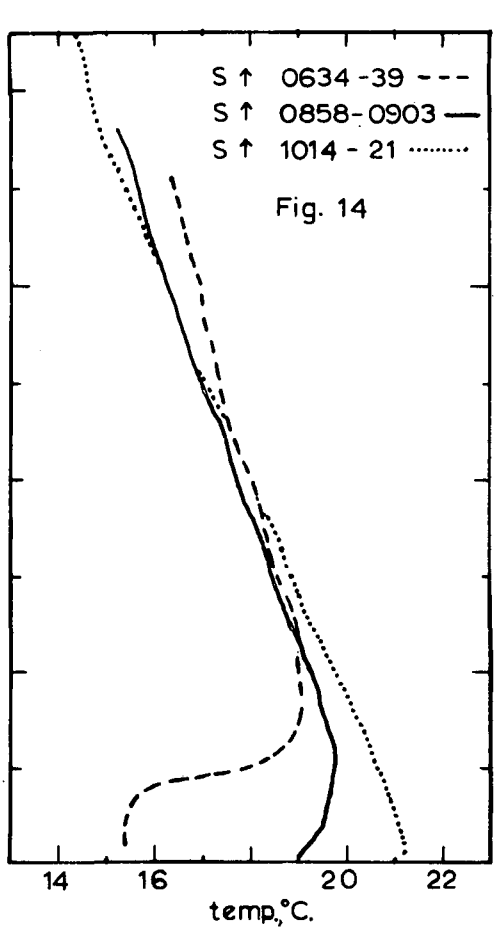

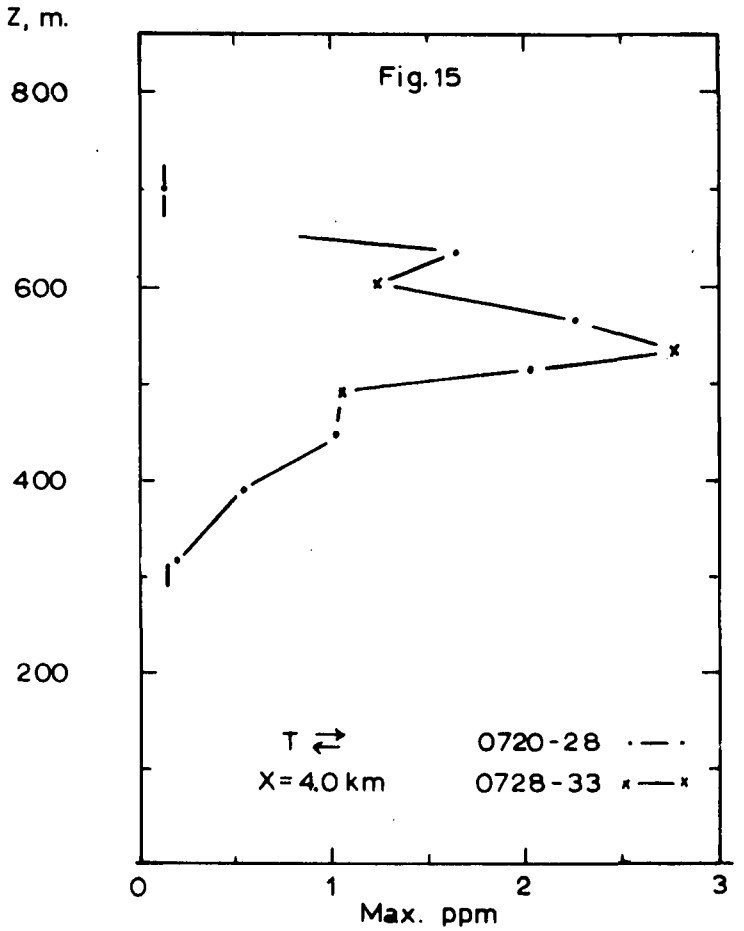

Z, m.
800
600
400
200

18 Oct. '68

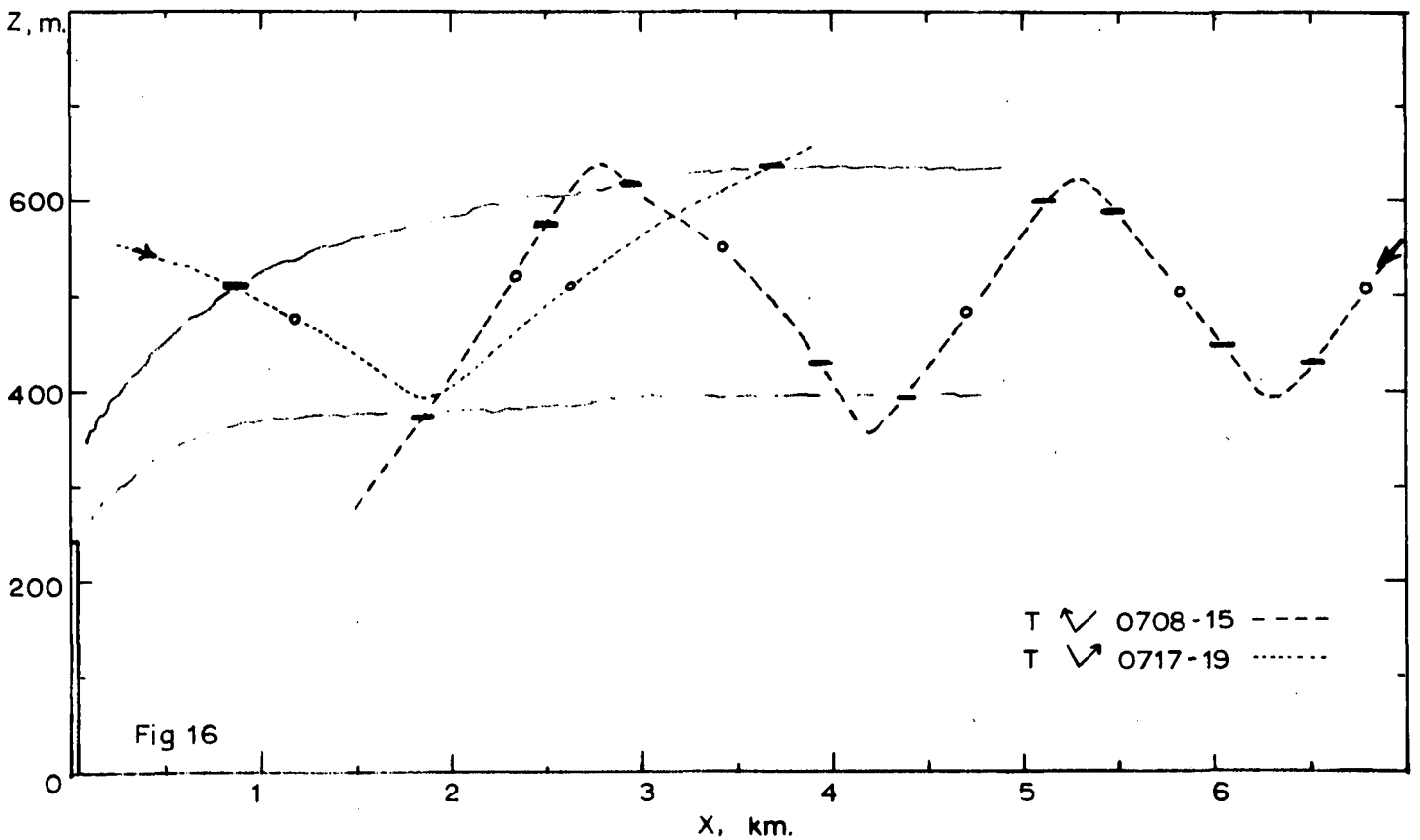

Date: 20 Oct. 68 Time: 0635-39 Type Traverse: ↖✓

Distance Downwind	Height of Top	Height of Bottom	Max. SO_2	Max. SO_2
km	m	m	m	ppm
4.6	460			
4.3			370	4.10
4.2		340		
3.7		350		
3.6			370	4.53
3.1	470			
2.3	480			
1.9			400	7.00
1.7		330		
1.5		320		
1.0			420	11.25
0.7	470			

Date: 20 Oct. 68 Time: 0654-59 Type Traverse: ↖✓

6.9	460			
6.8			430	2.32
6.4		340		
6.0		340		
5.5			420	3.70
5.1	460			
4.5	460			
4.1			380	4.18
3.9		330		
3.4		330		
2.8			440	5.64
2.6	480			
2.3	480			
1.7			350	(10.0+)
1.5		320		

Date: 20 Oct. 68 Time: 0701-02 Type Traverse: ↘

Distance Downwind	Height of Top	Height of Bottom	Height of Max. SO_2	Max. SO_2
km	m	m	m	ppm
0.3	470			
0.9			350	18.6
1.3		300		

Date: 20 Oct. 68 Time: 0706-13 Type Traverse: ↖↙

8.1	490			
8.0			460	2.85
7.5		350		
6.7		330		
6.1			430	3.60
5.9	460			
5.4	460			
5.0			400	3.60
4.6		300		
4.0		310		
3.6			370	4.88
3.1	460			
2.5	490			
2.3			440	4.23
1.7		320		
1.2		310		
1.0			390	8.40
0.6	450			

Date: 20 Oct. 68 Time: 0727-33 Type Traverse: ↖↙

7.6	460			
7.4			440	2.97
7.3		390		
6.3		390		
6.1			430	3.30
5.9	460			
5.4	460			
5.1			400	3.72
4.9		370		
4.0		380		
3.6			440	4.23
3.3	470			
2.8	470			
2.6			440	5.31
2.4		360		
1.8		320		
1.2			450	8.28
1.1	470			

Date: 20 Oct. 68 Time: 0903-08 Type Traverse: ↖✓

Distance Downwind	Height of Top	Height of Bottom	Height of Max. SO_2	Max. SO_2
km	m	m	m	ppm
6.8	520			
6.3			410	0.89
6.2		350		
5.0		360		
4.5			460	0.88
4.2	480			
3.9	500			
3.5			420	2.28
3.2		340		
2.6		330		
2.1			430	2.73
1.9	450			
1.5	450			
1.0			380	6.90
0.8		320		

Date: 20 Oct. 68 Time: 0927-32 Type Traverse: ↖✓

7.0	480			
6.9			450	3.42
6.4		380		
5.7		380		
5.5			400	3.56
5.1	450			
4.6	480			
4.4			440	3.80
4.1		370		
3.5		350		
3.1			420	3.04
2.4	480			
1.9	500			
1.3			410	5.13
1.0		350		

Date: 20 Oct. 68 Time: 0948-52 Type Traverse: ↖✓

Distance Downwind	Height of Top	Height of Bottom	Height of Max. SO_2	Max. SO_2
km	m	m	m	ppm
6.7	480			
6.5			450	1.38
6.0		360		
5.2		340		
4.3			460	2.18
4.1	480			
3.7	490			
3.6			460	2.37
3.2		370		
1.9		380		
1.3			470	3.48
.8	530			

Date: 20 Oct. 68 Time: 0953-54 Type Traverse: →

0.5	510			
1.2	500			
1.3	500			
2.5	500			

Date: 20 Oct. 68 Time: 1016-22 Type Traverse: ↖✓

9.2	630			
8.6			490	1.52
8.3		400		
7.5		390		
5.9	600			
5.6	620			
3.6		470		
2.8			600	1.83
2.7	630			
2.2	650			
1.9			590	2.48
1.2		470		

Date: 20 Oct. 68 Time: 0616-25 Type Traverse: ⇄

X = 4.0 km

Height, m ↓	Height, m ↑	Max. SO_2	Background SO_2
530		0.06	0.06
	500	0.06	0.06
470		2.27	
	450	3.53	
420		3.13	
	380	2.96	
340		0.26	
320		0.14	0.09

Date: 20 Oct. 68 Time: 0642-51 Type Traverse: ⇄

X = 4.0 km

Height, m ↓	Height, m ↑	Max. SO_2	Background SO_2
500		0.05	0.05
	480	1.40	
440		2.28	
	420	3.52	
380		4.80	
	350	1.90	
310		0.09	0.09

Date: 20 Oct. 68 Time: 0911-24 Type Traverse: ⇄

X = 4.0 km

Height, m ↓	Height, m ↑	Max. SO_2	Background SO_2
	500	0.10	0.10
520		0.10	
	470	4.92	
440		3.55	
	410	2.65	
370		1.13	
	340	0.43	
310		0.37	
280		0.35	0.16

Date: 20 Oct. 68 Time: 0935-45 Type Traverse: ⇄

X = 2.9 km

↓	↑		
240		0.18	0.18
310		0.18	
	340	0.42	
370		0.63	
	410	1.12	
440		3.66	
	470	2.64	
500		0.22	0.10

Date: 20 Oct. 68 Time: 0956-1013 Type Traverse: ⇄

X = 4.1 km

↓	↑		
610		0.11	0.11
	600	0.39	
	530	1.36	
490		1.69	
	480	2.57	
440		2.41	
	410	1.82	
370		1.98	
	350	0.37	
310		0.31	
280		0.24	0.19

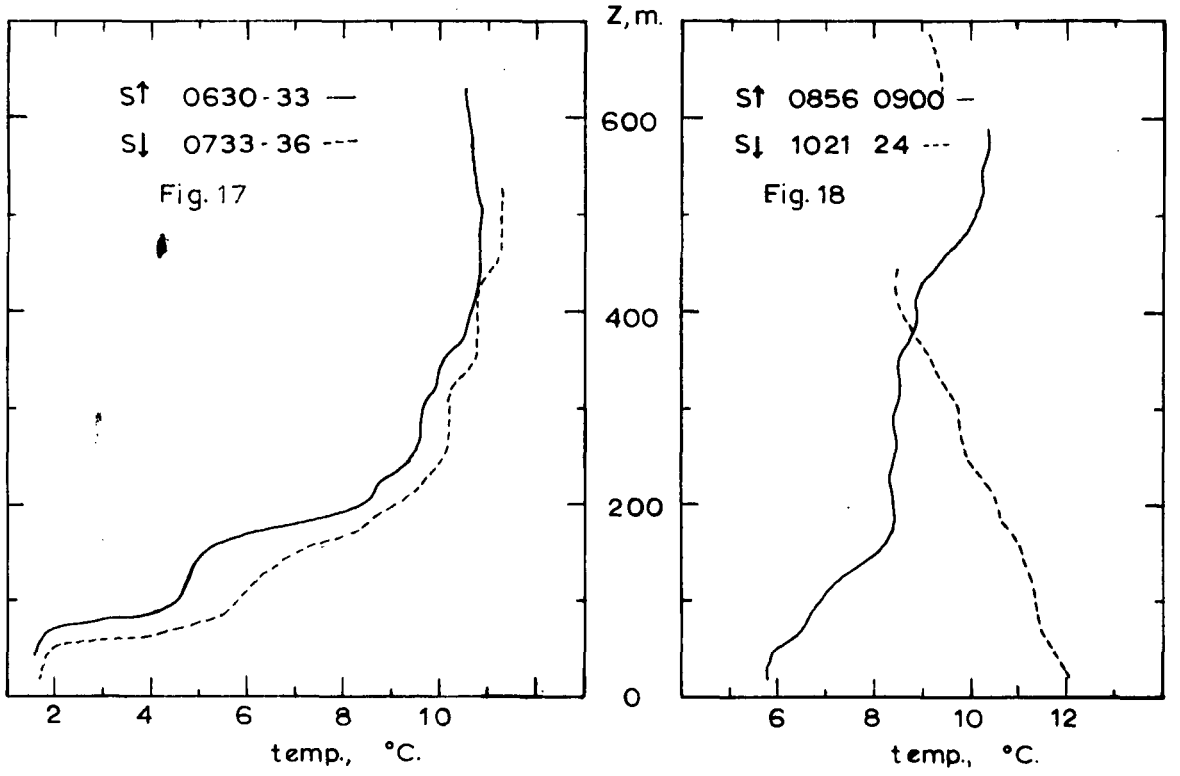
S↑ 0630-33 —
S↓ 0733-36 ---
Fig. 17
Z, m.
600
400
200
0
2
4
6
8
10
temp., °C.
S↑ 0856 0900 –
S↓ 1021 24 ---
Fig. 18
6
8
10
12
temp., °C.

20 Oct. '68

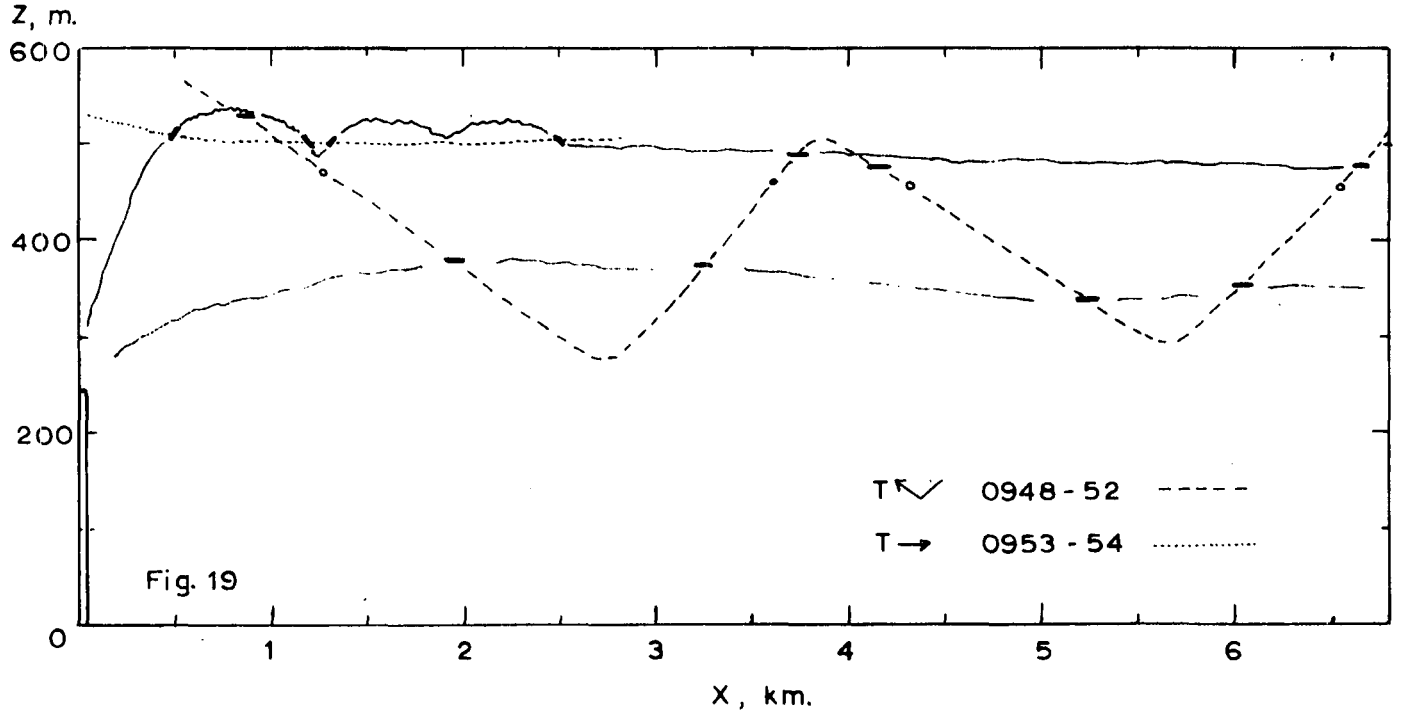
Z, m.
600
400
200
0
T↖↙ 0948-52 -----
T→ 0953-54 .....
Fig. 19
1
2
3
4
5
6
X, km.

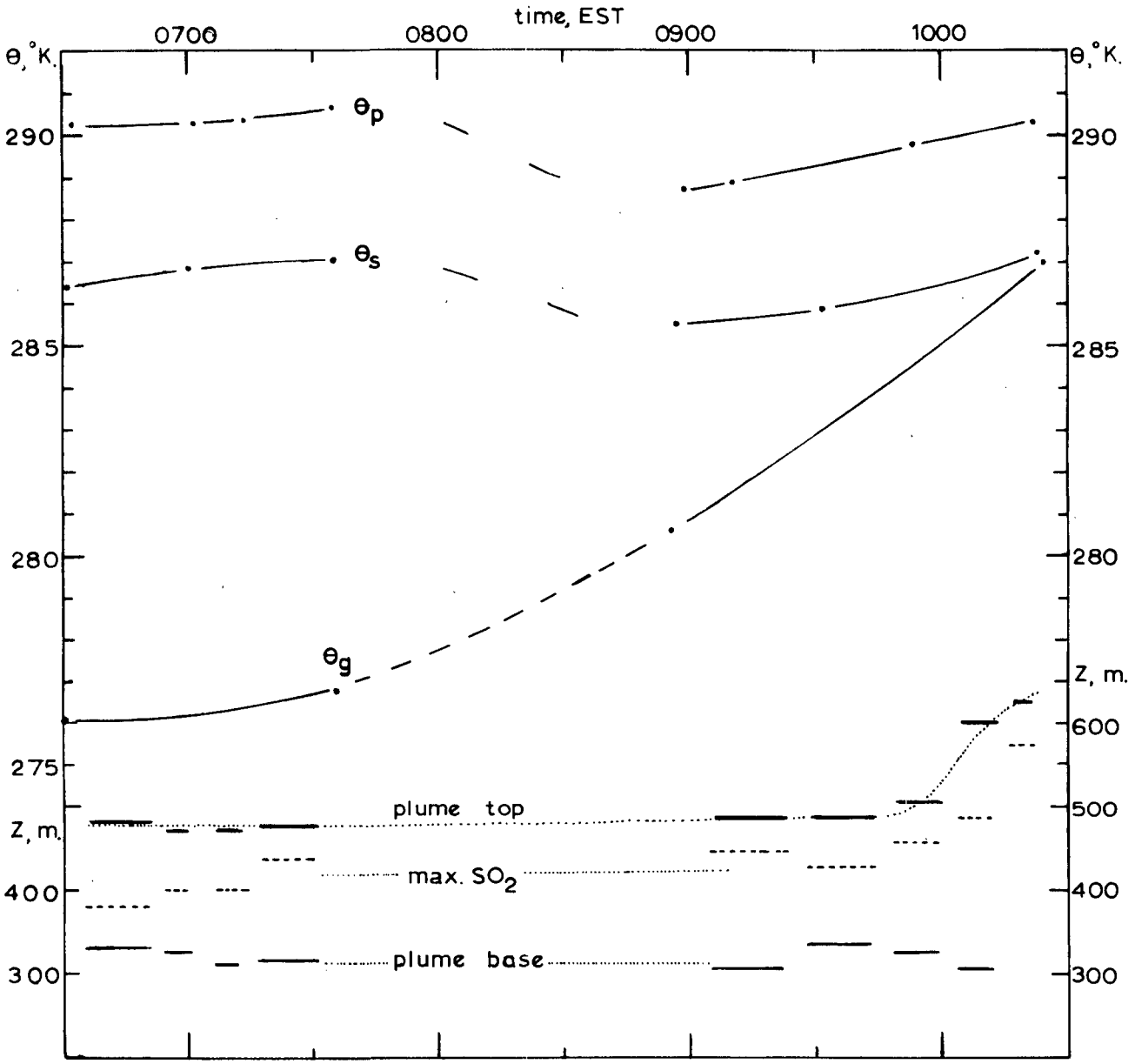

FIG.20. Potential temperatures at plume top, θ_p, stack top, θ_s, and stack base level plus 20 m., θ_g, as a function of time. Plume heights were obtained from horizontal and slanting traverses. The first flight was from 0630 to 0745 EST and the second from 0900 to 1030 EST, 20 October 1968.

FIG. 21 (below). Isolines of SO_2, drawn from a series of seven horizontal traverses between 0642-51 EST, 20 October, 1968.

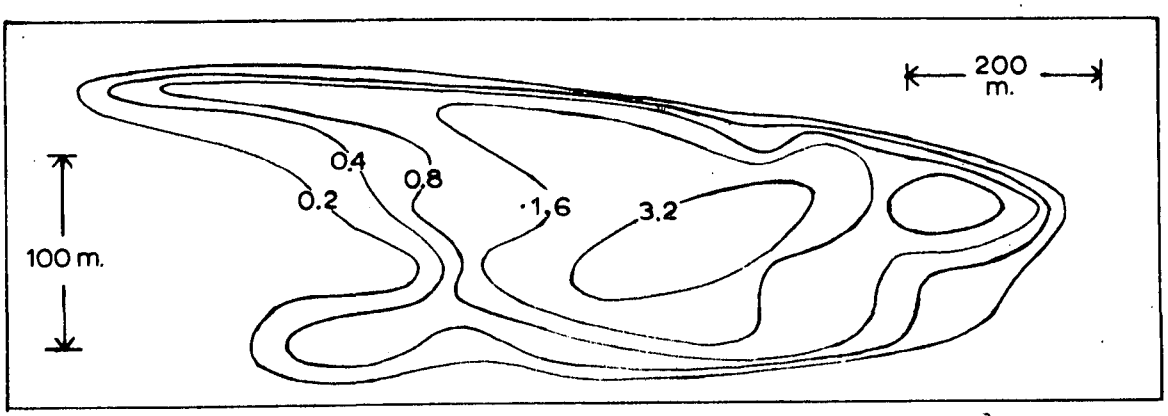

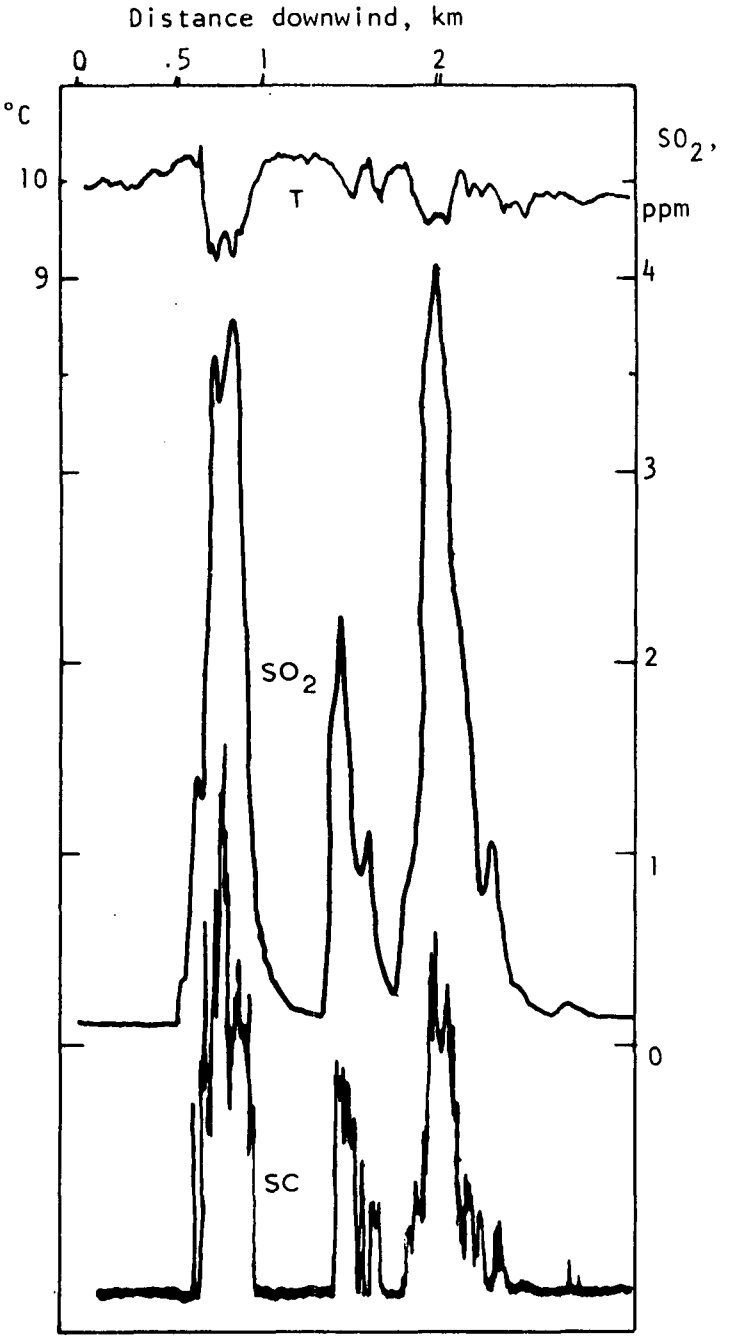

Fig. 22
Traces of temperature, SO_2, and space charge derivative recorded while making a constant level traverse, at 510 m., from over the stack downwind to about 2.5 km. The traverse was made through the top of the plume and shows a temperature deficit of about 1.0°C, indicating plume overshoot. Time: 0954 EST, 20 Oct. 68.

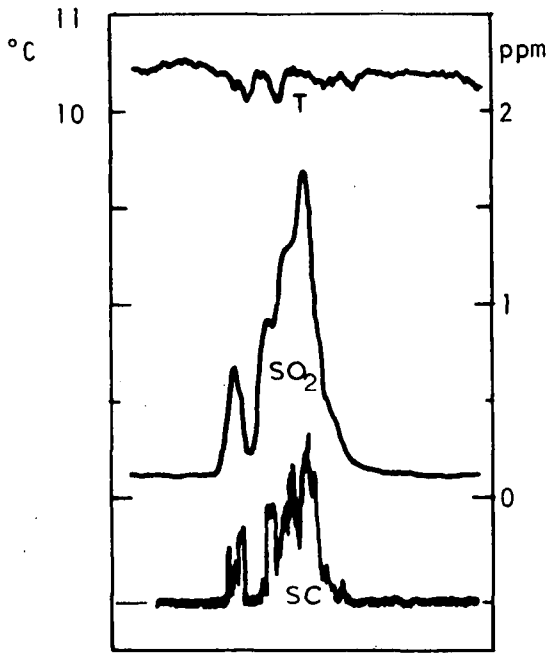

Fig. 23
Temperature, SO_2, and space charge derivative recorded during a horizontal traverse through, and normal to, the plume at a distance of 4.1 km. downwind. Height = 490 m. Space charge device indicates positively charged particles in the plume. Time: 0957 EST, 20 Oct. 68.

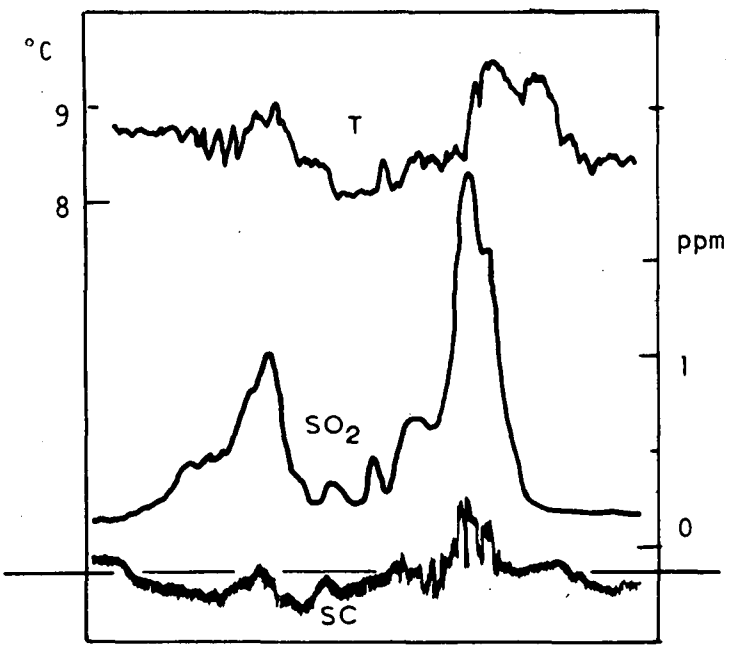

Fig. 24

Temperature, SO_2, and space charge derivative recorded during a horizontal traverse through the plume at a height of 370 m. and distance of 4.1 km. Time: 1000 EST, 20 Oct. 68. The space charge device indicates the presence of both positive and negative particles, the latter probably from the cooling tower plume.

(Note: Flights through the cooling tower plume have shown negative charge - opposite to that in the main SO_2 plume. Twenty-five minutes after the above traverse, a pass was made through the moisture plume, 150 meters above the cooling tower - roughly the height of the main stack. The space charge device went off scale, negatively, and the temperature trace showed an increase of 12°C. Taking the time constant of the temperature transducer and the recorder into account, the increase would be a degree or two higher; the virtual temperature increment was about 4°C. Therefore the effective temperature difference was about 17-18°C above ambient.)

Date: 21 Oct. 68 Time: 0640-45 Type Traverse: ↖✓

Distance Downwind	Height of Top	Height of Bottom	Height of Max. SO_2	Max. SO_2
km	m	m	m	ppm
5.1			610	2.42
4.1		410		
3.7			500	3.19
3.2	600			
2.5	570			
2.0			480	4.49
1.6		400		
1.1		390		
0.9			430	6.94
0.4	560			

Date: 21 Oct. 68 Time: 0702-10 Type Traverse: ↖✓

6.8		440		
6.1		460		
5.9			510	2.11
4.9	680			
3.9			490	3.13
3.1		340		
2.5			420	4.59
1.4	630			

Date: 21 Oct. 68 Time: 0715-21 Type Traverse: ↖✓

7.6	710			
6.9			550	1.45
6.5		490		
5.7		480		
4.9			690	2.98
4.7	740			
4.3	740			
3.4			530	3.26
2.9		410		
2.7			440	5.23
1.9			580	4.15
1.7	620			

Date: 21 Oct. 68 Time: 0723 Type Traverse: ↘

Distance Downwind	Height of Top	Height of Bottom	Height of Max. SO_2	Max. SO_2
km	m	m	m	ppm
0.6	490			
0.7			480	8.40
1.2		400		

Date: 21 Oct. 68 Time: 0908-14 Type Traverse: ↖↙

7.4	910			
6.2			570	2.02
5.6		370		
4.3			550	2.65
3.7	670			
2.7			430	2.99
2.0		260		
0.9			520	5.98
0.8	550			

Date: 21 Oct. 68 Time: 0915-16 Type Traverse: ↘

1.1	510			
1.3			480	6.14
2.8		230		

Date: 21 Oct. 68 Time: 0918-22 Type Traverse: ↖↙

4.7		280		
3.5			570	2.56
2.8	680			
2.0			540	4.38
1.1		330		

Date: 21 Oct. 68 Time: 0648-59 Type Traverse ⇄

X = 3.3 km

Height, m ↓	Height, m ↑	Max. SO_2	Background SO_2
700		0.07	0.07
630		1.02	
	600	0.07	
580		2.06	
	550	1.08	
520		1.68	
	500	3.86	
460		1.11	
390		0.60	
340		0.07	0.07

Date: 21 Oct. 68 Time: 0725-37 Type Traverse ⇄

X = 3.3 km

Height, m ↑	Height, m ↓	Max. SO_2	Background SO_2
320		0.10	0.10
	360	0.10	
390		0.50	
	420	1.20	
450		1.59	
	480	2.46	
520		2.24	
	550	2.38	
580		3.80	
	600	2.76	
630		1.70	
690		0.10	0.10

Date: 21 Oct. 68 Time: 0853-0904 Type Traverse: ⇄

X = 4.0 km

Height, m ↓	Max. SO_2	Background SO_2
930	0.19	0.08
900	0.78	
830	1.81	
760	2.28	
690	2.71	
630	1.19	
560	1.14	
510	0.27	
450	0.32	0.10

Date: 21 Oct. 68 Time: 1005-18 Type Traverse: ⇄

X = 4.2 km

↓		
880	0.10	0.10
820	2.09	
760	0.80	
700	1.26	
630	1.81	
560	0.95	
510	0.38	
440	0.31	
380	1.10	
310	0.38	0.11

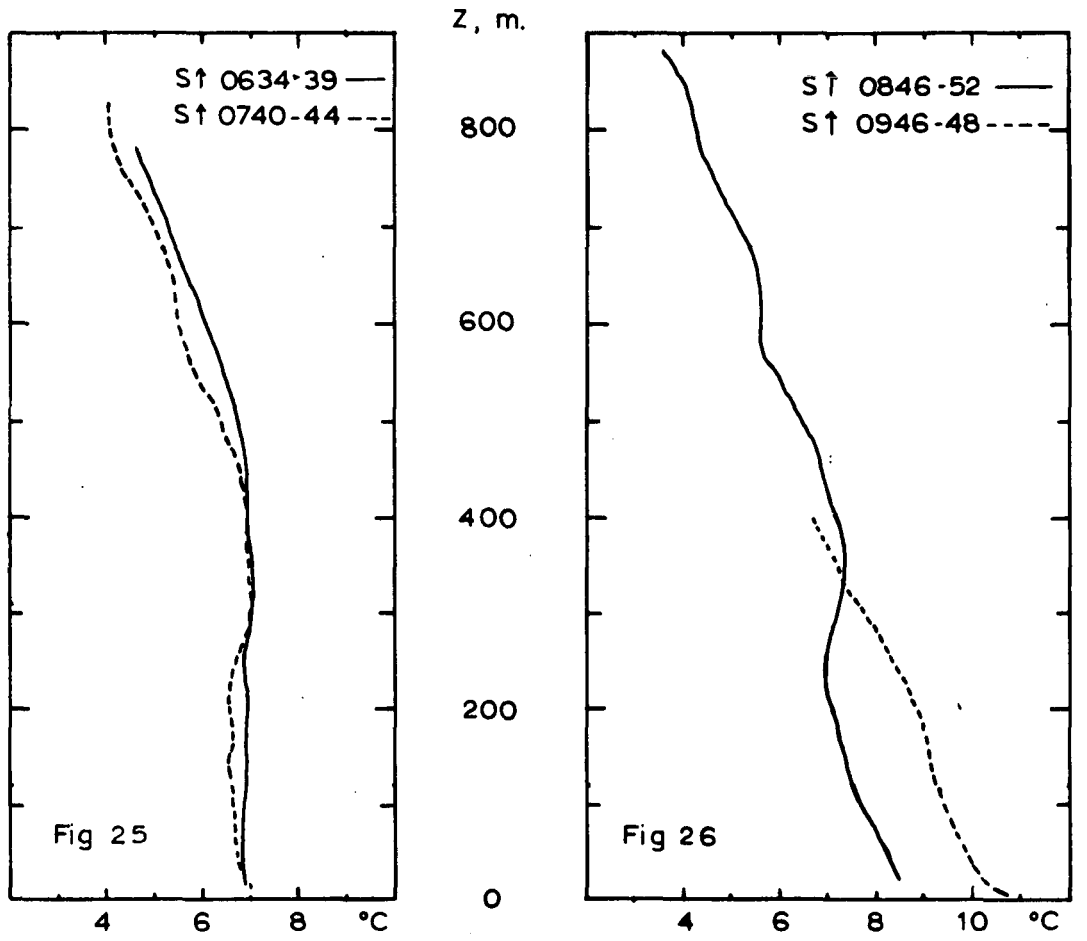
Z, m.
S↑ 0634-39
S↑ 0740-44
S↑ 0846-52
S↑ 0946-48
800
600
400
200
0
4
6
8
°C
10
Fig 25
Fig 26

21 Oct. '68

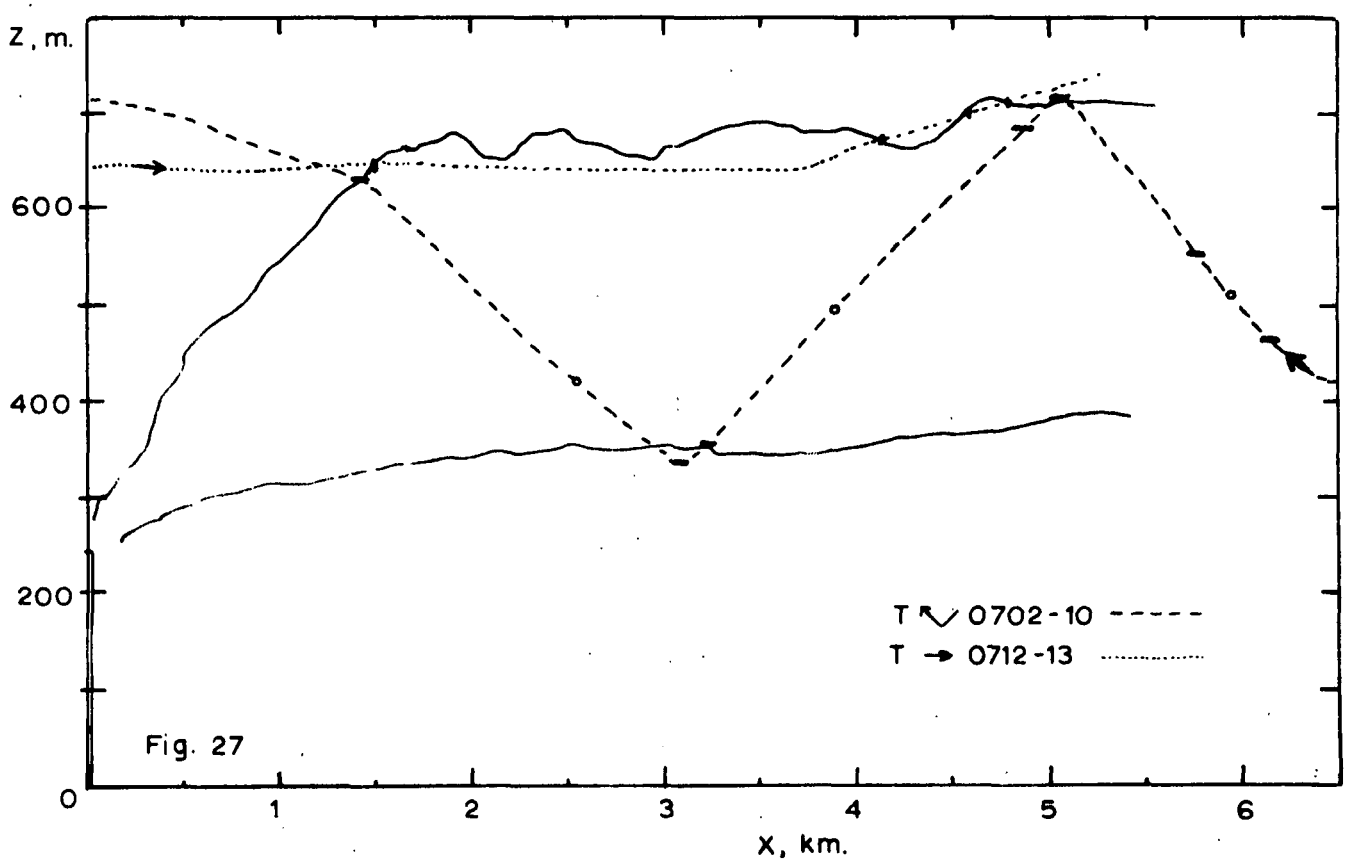
Z, m.
600
400
200
0
1
2
3
4
5
6
X, km.
T ↘ 0702-10
T → 0712-13
Fig. 27

Date: 22 Oct. 68 Time: 0644-50 Type Traverse: ↖✓

Distance Downwind	Height of Top	Height of Bottom	Height of Max. SO_2	Max. SO_2
km	m	m	m	ppm
7.5	480			
7.4			450	0.80
7.2		380		
4.8		380		
4.2			450	2.04
4.0	470			
3.2	490			
3.0			460	2.77
2.7		390		
1.8		350		
1.6			390	5.78
1.0	470			

Date: 22 Oct. 68 Time: 0654-58 Type Traverse: ↖✓

5.4	490			
5.3			460	1.96
5.1		410		
4.2		390		
4.0			430	3.12
3.6	480			
2.9	490			
2.2		350		
1.5		350		
1.1			410	6.34
0.7	470			

Date: 22 Oct. 68 Time: 0718-24 Type Traverse: ↖↙

Distance Downwind	Height of Top	Height of Bottom	Max. SO_2	Max. SO_2
km	m	m	m	ppm
6.9	510			
6.5			410	3.38
6.4		480		
5.5		480		
5.0			450	3.33
4.8	490			
4.2	500			
3.9			430	1.92
3.7		370		
2.8		360		
2.7			380	3.39
2.4	440			
1.8	470			
1.7			440	4.88
1.3		320		

Date: 22 Oct. 68 Time: 0903-0910 Type Traverse: ↖↙

7.1	490			
7.0			450	2.70
6.8		380		
5.7		380		
5.3			440	3.64
4.7	520			
3.7	520			
3.5			480	4.00
3.0		350		
2.5		350		
1.9			450	(10.0+)
1.4	530			

Date: 22 Oct. 68 Time: 0911-0913 Type Traverse: ↙↗

0.8	500			
1.2			430	9.03
1.6		340		
2.6		380		
3.4			470	4.33
3.9	540			

Date: 22 Oct. 68 Time: 0932-0940 Type Traverse: ↖↙

Distance Downwind	Height of Top	Height of Bottom	Height of Max. SO_2	Max. SO_2
km	m	m	m	ppm
9.6	610			
9.3			540	4.21
8.6		380		
8.1		360		
7.2			490	2.99
6.5	600			
6.1	640			
5.7			550	2.79
5.0		370		
4.4		360		
3.3			560	4.17
3.1	610			
2.7	620			
2.1			460	6.96
1.8		370		
1.6		350		
1.1			520	(10.0+)
1.0	550			

Date: 22 Oct. 68 Time: 1000-1008 Type Traverse: ↖↙

9.8	600			
9.4			480	3.23
9.1		390		
8.3		380		
7.8			450	3.86
7.3	520			
6.7	530			
6.5			480	3.12
6.3		410		
5.5		360		
5.1			420	2.31
4.6	520			
3.8	490			
3.8			480	3.38
3.4		350		
3.1		320		
1.7			570	6.16
1.5	590			

Date: 22 Oct. 68 Time: 0700-0715 Type Traverse: ⇄

X = 3.4 km

Height, m ↓	Height, m ↑	Max. SO_2	Background SO_2
	610	0.08	0.08
580		0.74	
	540	2.58	
510		2.26	
	480	3.33	
450		2.32	
	420	3.06	
380		2.50	
	360	1.32	
320		0.13	0.07

Date: 22 Oct. 68 Time: 0726-0740 Type Traverse: ⇄

X = 3.4 km

Height, m ↑	Height, m ↓	Max. SO_2	Background SO_2
250		0.10	0.09
	280	0.10	
320		1.56	
	340	1.22	
380		2.87	
	420	4.00	
460		3.35	
	480	1.73	
510		0.70	
	580	0.08	0.08

Date: 22 Oct. 68 Time: 0915-29 Type Traverse: ⇄

X = 3.4 km

Height, m ↓	Height, m ↑	Max. SO_2	Background SO_2
620		0.11	0.11
	600	0.11	
570		3.18	
	530	2.26	
490		3.49	
	460	3.32	
450		1.01	
	420	1.70	
370		1.19	
	340	0.21	
310		0.12	0.12

Date: 22 Oct. 68 Time: 0945-57 Type Traverse: ⇄

X = 4.8 km

Height, m ↓	Height, m ↑	Max. SO_2	Background SO_2
560		0.13	0.13
	520	0.94	
490		0.94	
	480	5.20	
440		3.18	
360		1.23	
	330	0.39	
310		0.20	0.17

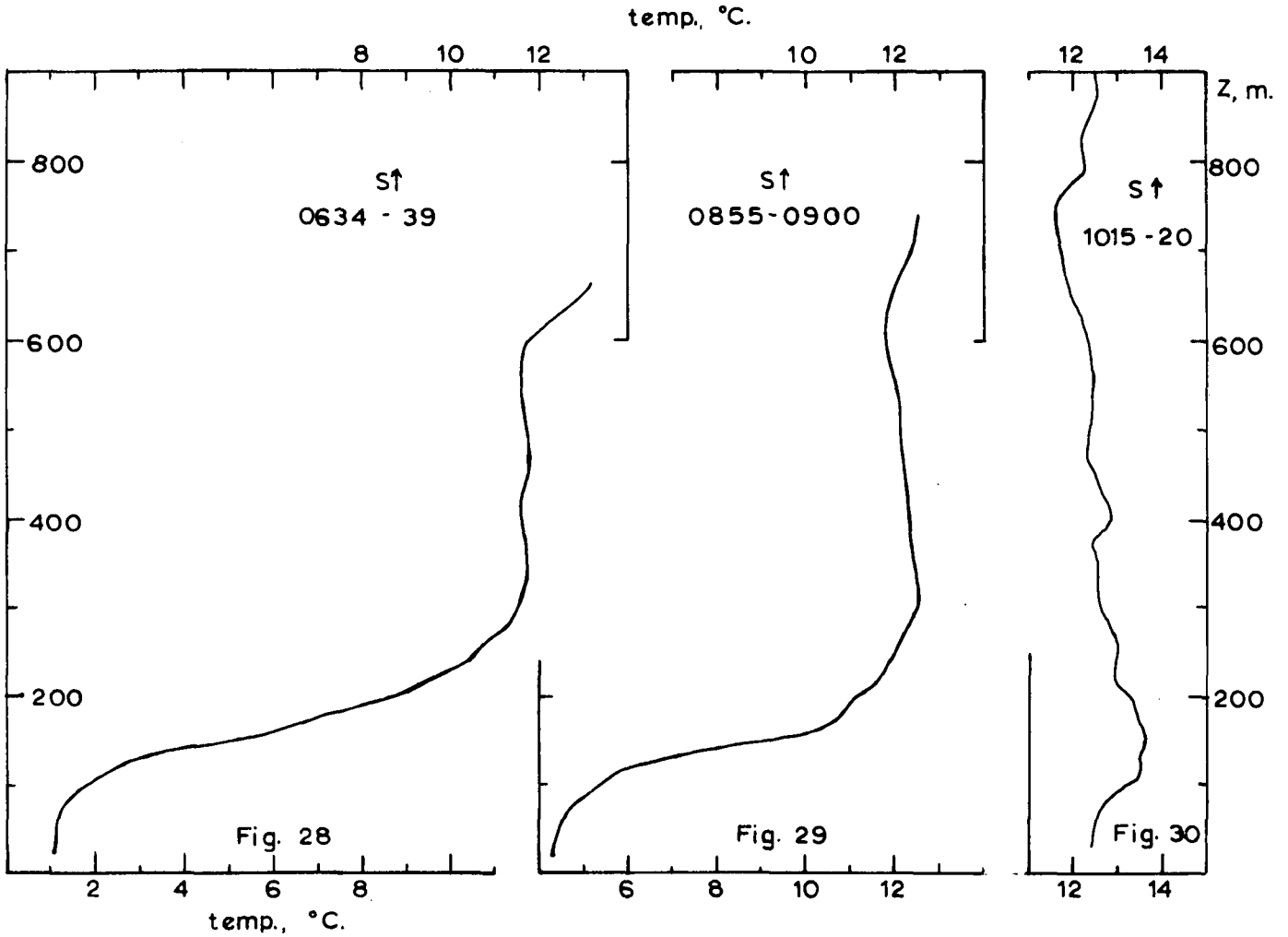
temp., °C.
8 10 12
800
600
400
200
S↑
0634 - 39
Fig. 28
2 4 6 8
temp., °C.
10 12
S↑
0855-0900
Fig. 29
6 8 10 12
12 14
Z, m.
800
600
400
200
S↑
1015 - 20
Fig. 30
12 14

22 Oct. '68

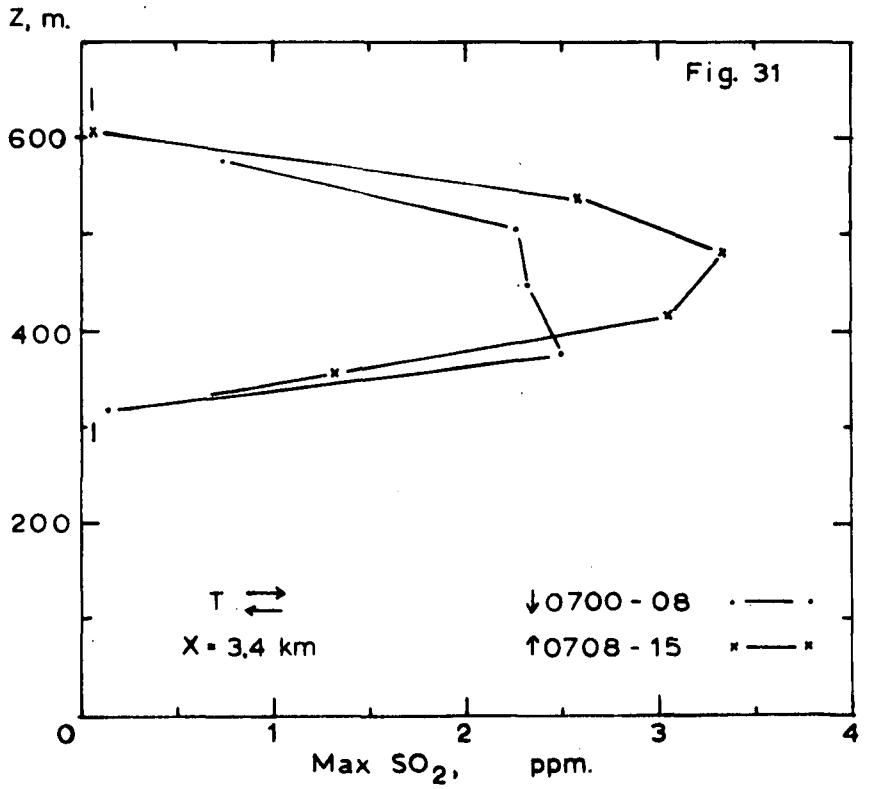
Z, m.
Fig. 31
600
400
200
0
1
2
3
4
T ⇄
X = 3.4 km
↓0700 - 08
↑0708 - 15
Max SO_2, ppm.

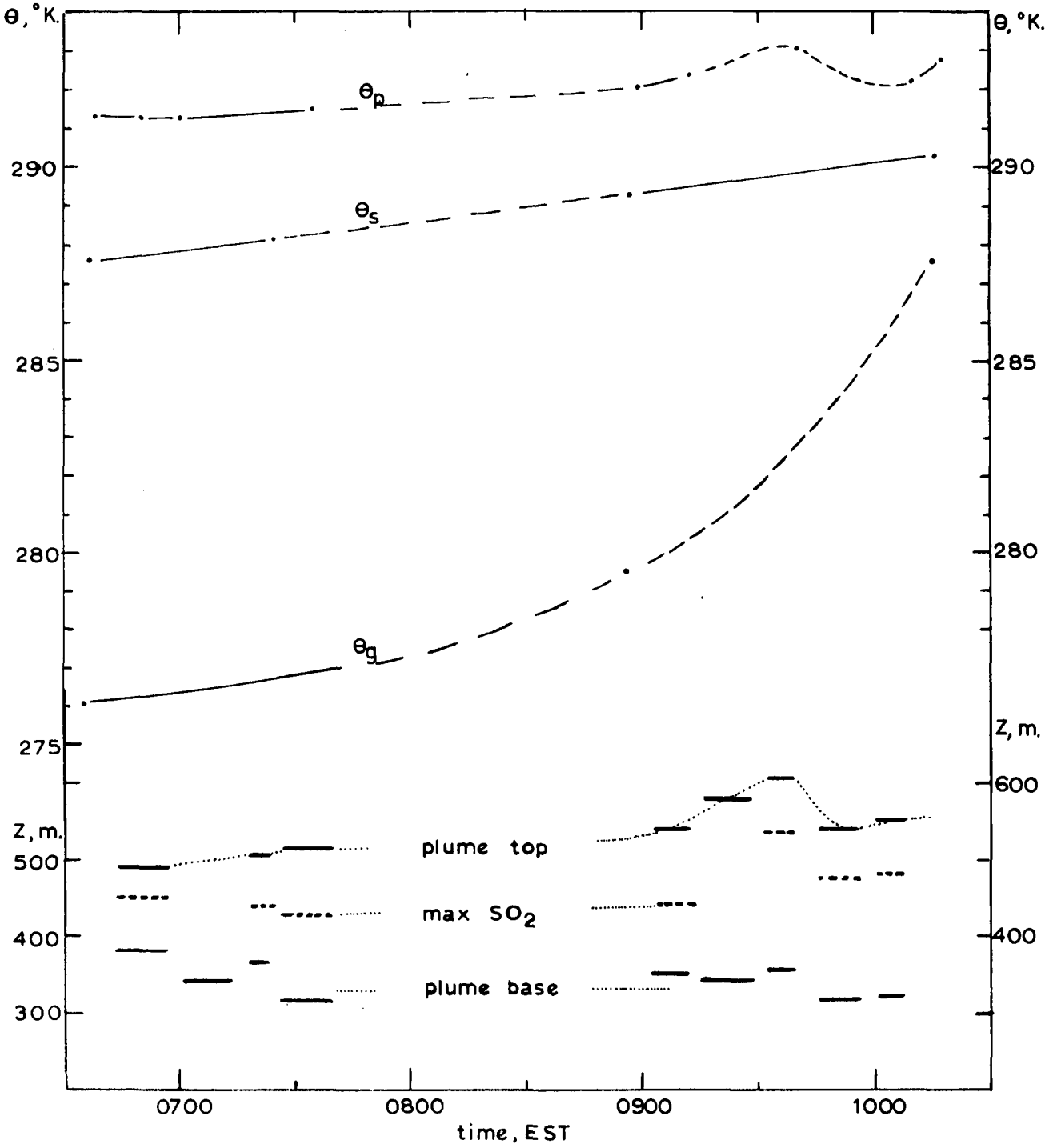

Fig. 32

22 October 1968

Potential temperatures at plume top, θ_p, stack top, θ_s, and stack base level plus 20 m., θ_g, as a function of time. Heights of plume top, base and maximum SO_2 concentration are shown vs time. The first flight was from 0630 to 0745 EST and the second from 0900 to 1030.

Date: 23 Oct. 68 Time: 0641-50 Type Traverse: ↖✓

Distance Downwind	Height of Top	Height of Bottom	Max. SO_2	Max. SO_2
km	m	m	m	ppm
7.1	610			
6.9			500	0.76
6.7		430		
5.9		420		
5.5			510	(1.0+)
5.1	650			
4.6	650			
4.2			500	1.41
4.1		470		
3.6		410		
3.2			550	2.55
2.9	650			
2.4	630			
2.1			500	4.57
1.9		410		
1.6		370		
1.3			480	5.04
1.1	530			

Date: 23 Oct. 68 Time: 0710-20 Type Traverse ↖✓

7.5			510	0.50
6.6		400		
6.4			450	0.91
6.0	580			
5.7	610			
5.1			440	1.30
4.9		400		
4.3		400		
3.7			540	1.78
3.4	630			
2.8	640			
2.2			470	3.57
2.0		400		
1.4		410		
1.1			470	6.77
1.0	490			

Date: 23 Oct. 68 Time: 0908-15 Type Traverse: ↖✓

Distance Downwind	Height of Top	Height of Bottom	Max. SO_2	Max. SO_2
km	m	m	m	ppm
7.1	900			
6.2			650	0.38
5.6		460		
3.8		420		
2.7			750	1.53
2.1	920			
1.5	810			
0.6			450	4.77
0.3		350		

Date: 23 Oct. 68 Time: 0941-48 Type Traverse: ↖✓

6.4		400		
5.1		330		
3.9			610	1.11
2.9			840	1.18
2.1	1060			

Date: 23 Oct. 68 Time: 0653-0707 Type Traverse: ⇄

X = 4.0 km

Height, m ↑	Max. SO_2	Background SO_2
250	0.20	0.08
310	0.39	
380	0.43	
440	1.62	
500	1.56	
560	1.38	
630	1.01	
690	0.06	0.06

Date: 23 Oct. 68 Time: 0723-42 Type Traverse: ⇄

X = 2.0 km

↑	↓		
	160	0.11	0.12
	220	0.38	
	290	0.39	
310		0.70	
	350	0.52	
390		0.83	
	420	0.63	
450		1.53	
	480	2.56	
500		2.83	
	530	2.89	
580		2.33	
630		0.94	
700		0.08	0.08

Date: 23 Oct. 68 Time: 0917-37 Type Traverse: ⇄

X = 2.1 km

Height, m ↑	Max. SO_2	Background SO_2
250	0.20	0.12
310	0.94	
380	0.48	
450	1.08	
520	0.73	
570	1.74	
640	1.87	
690	2.52	
760	0.52	
830	1.12	
880	0.68	
950	0.72	
1020	0.10	0.10

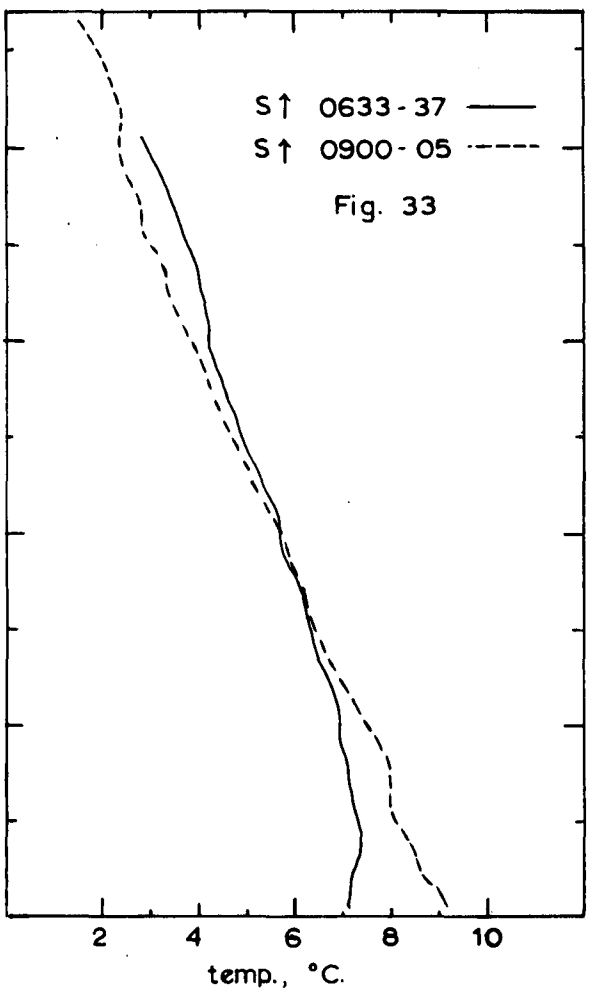
S↑ 0633-37
S↑ 0900-05
Fig. 33
2
4
6
8
10
temp., °C.

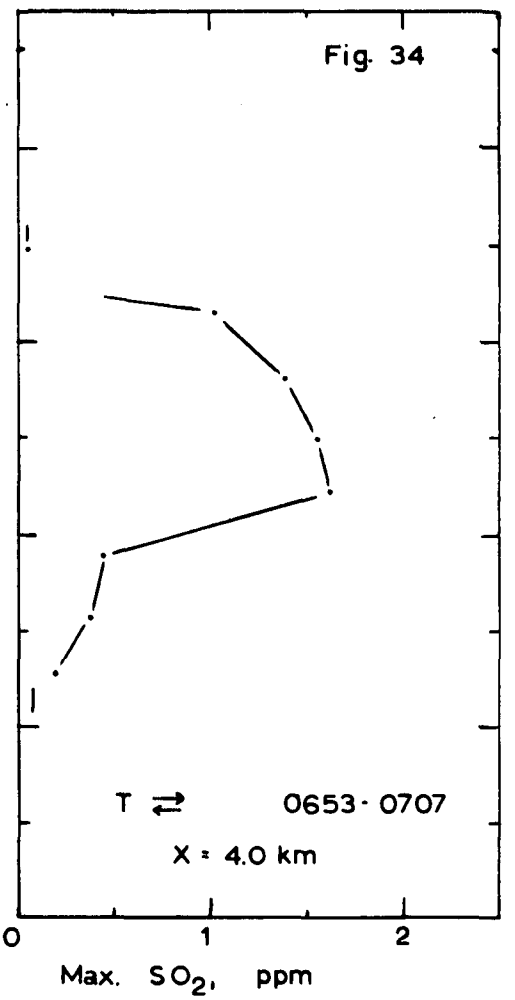
Z, m.
800
600
400
200
Fig. 34
T ⇄ 0653-0707
X = 4.0 km
0
1
2
Max. SO_2, ppm

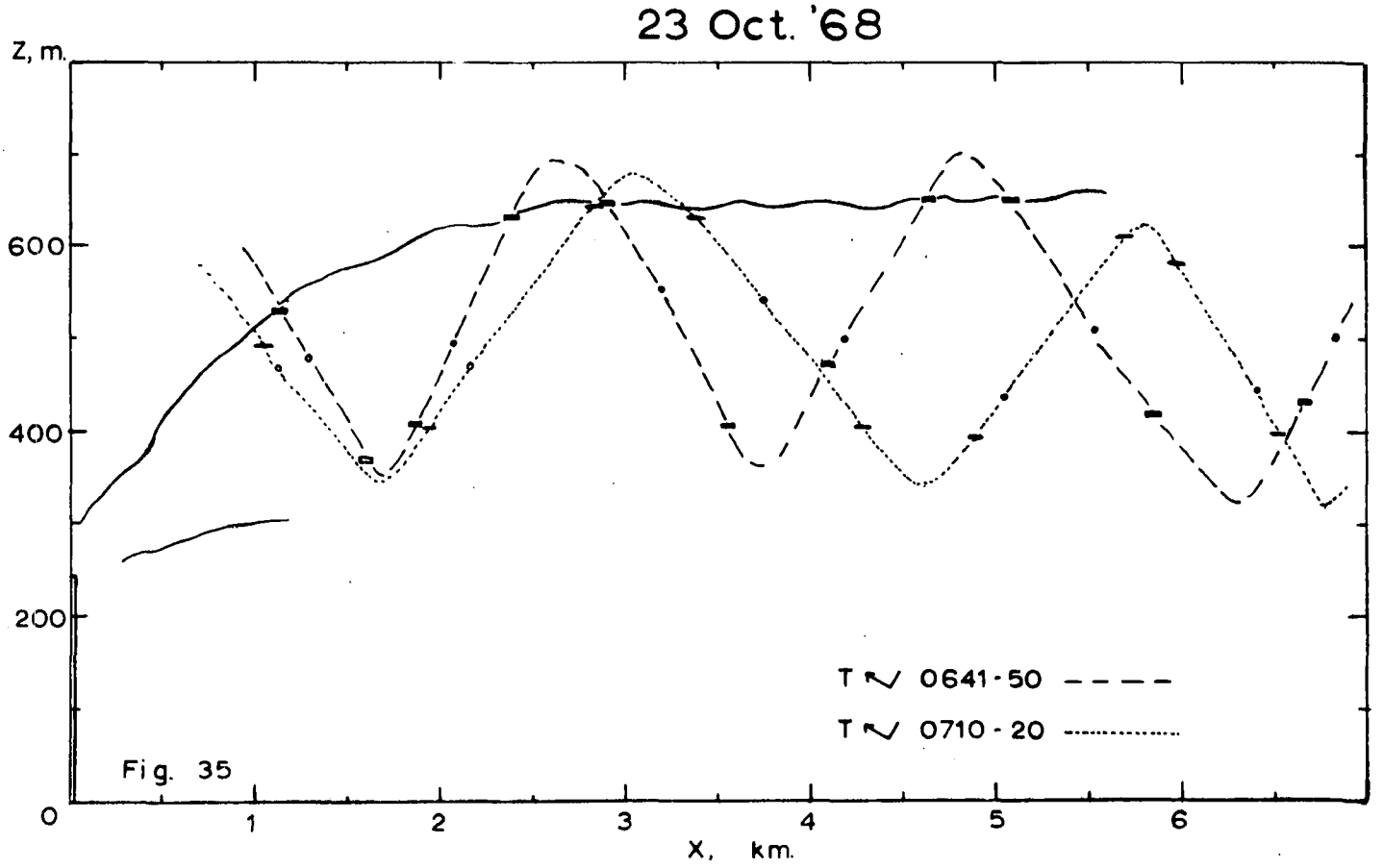
23 Oct. '68
Z, m.
600
400
200
T ↖↘ 0641-50
T ↖↘ 0710-20
Fig. 35
0
1
2
3
4
5
6
X, km.

Date: 24 Oct. 68 Time: 0645-50 Type Traverse: ↖↙

Distance Downwind	Height of Top	Height of Bottom	Height of Max. SO_2	Max. SO_2
km	m	m	m	ppm
6.4	950			
4.9			640	1.29
4.4		500		
3.3		500		
2.1			790	2.57
1.7	890			

Date: 24 Oct. 68 Time: 0717-21 Type Traverse: ↖↙

4.3		520		
3.4			700	2.02
2.5	880			
1.2			520	8.18

Date: 24 Oct. 68 Time: 0736-38 Type Traverse: ↙

3.6	970			
2.4			660	2.17
1.5		440		

Date: 24 Oct. 68 Time: 0655-0714 Type Traverse: ⇄

X = 4.0 km

Height, m ↑	Max. SO_2	Background SO_2
390	0.11	0.07
470	0.14	
520	0.62	
580	0.59	
640	1.36	
710	1.50	
780	1.67	
840	1.15	
900	1.94	
960	1.83	
1020	0.86	
1070	0.05	0.05

Date: 24 Oct. 68 Time: 0723-35 Type Traverse: ⇄

X = 2.5 km

↑		
390	0.09	0.08
460	0.32	
520	1.40	
580	2.24	
640	3.13	
710	2.75	
760	2.19	
840	2.20	
890	0.06	0.06

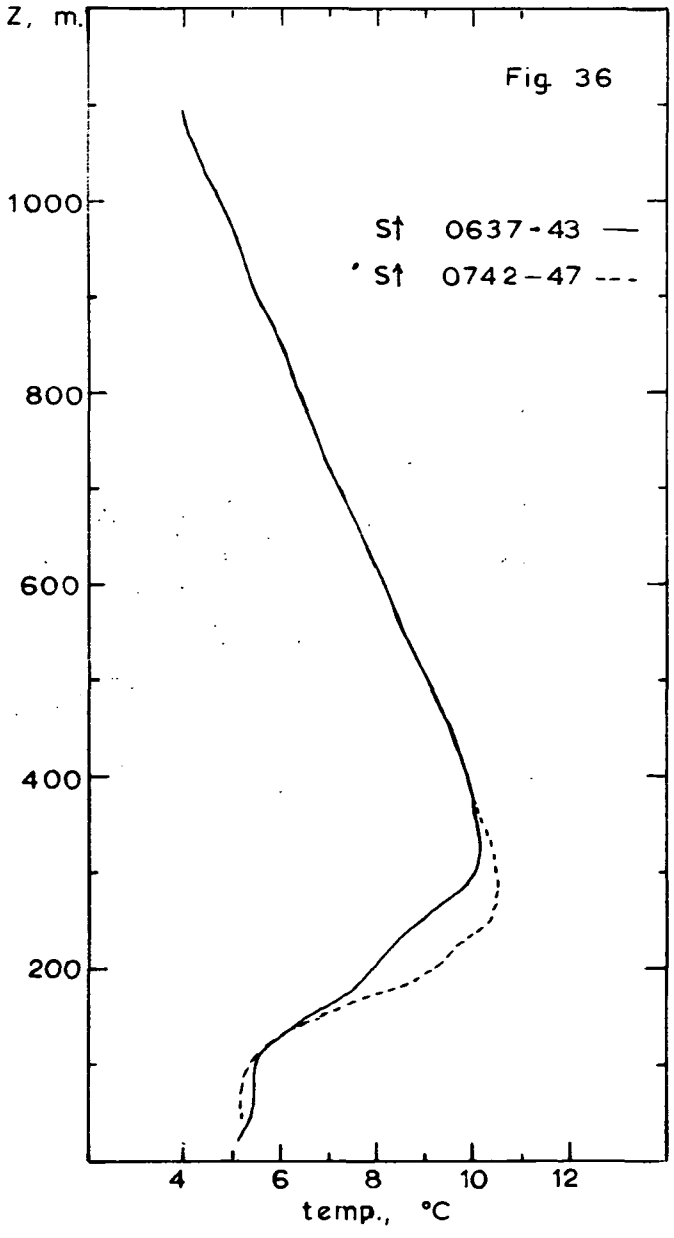
Z, m.
Fig. 36
1000
800
600
400
200
St 0637-43
St 0742-47
4
6
8
10
12
temp., °C

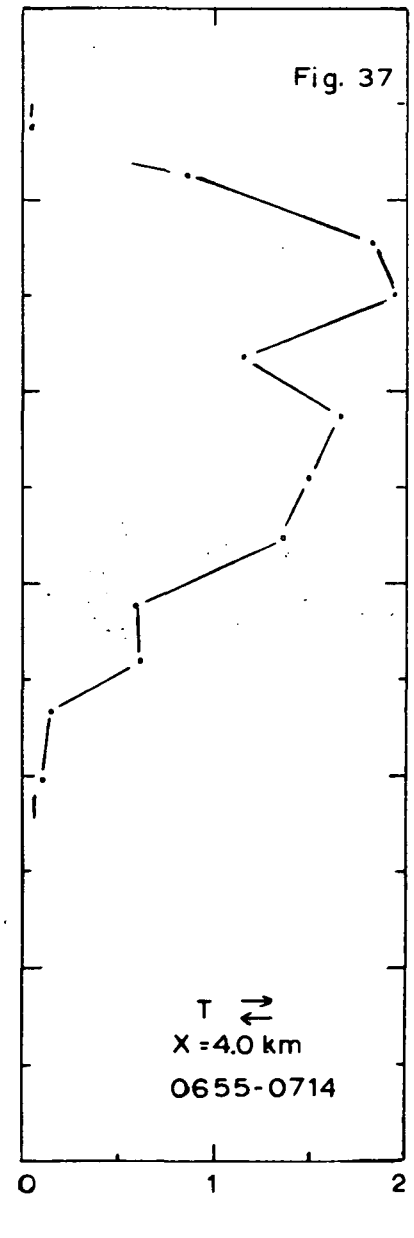
Fig. 37
T
X = 4.0 km
0655-0714
0
1
2

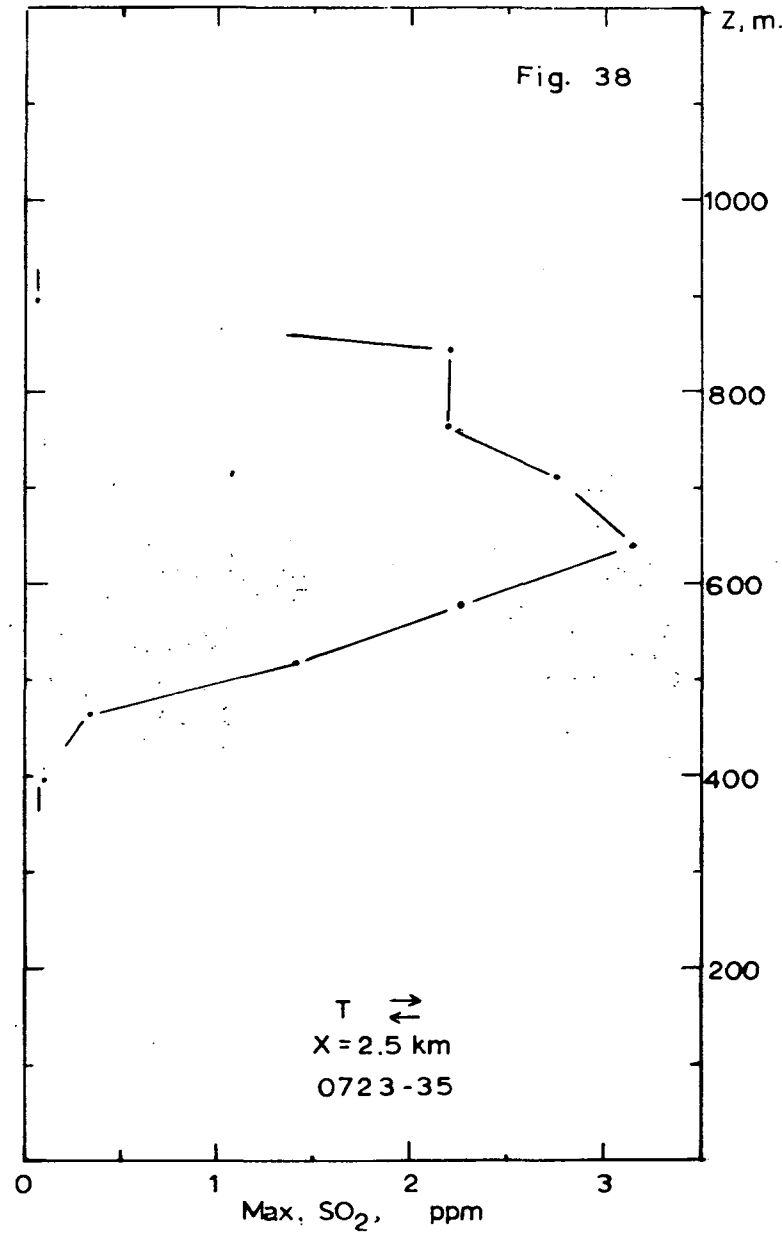
Z, m.
Fig. 38
1000
800
600
400
200
T
X = 2.5 km
0723-35
0
1
2
3
Max, SO_2, ppm

24 Oct. '68

PART III - ANALYSIS

BEHAVIOUR OF HOT PLUMES UNDER STABLE CONDITIONS[1/]

Betsy Woodward Proudfit[2/]

ABSTRACT

Using an instrumented helicopter, measurements have been made of the Keystone plant near Indiana, Penn. The data show that plume rise is primarily a function of stability in a highly stable environment. As the environmental stability decreases the effect of the mean wind speed on the plume rise increases. It is argued that values for the mean wind speed and average stability in the vertical region from stack top to plume top be used when predicting plume rise. The term, $\Delta\theta$, the difference in potential temperature between stack top and plume top, is introduced. Employing the concept that $\Delta\theta$ is the maximum potential temperature difference that can be penetrated, it is shown how plume rise can be estimated easily and quickly with the aid of diagrams.

1/ Paper No. ICFTC-NAFTC-4 sponsored by the Institute of Combustion and Fuel Technology of Canada for presentation at the NORTH AMERICAN FUEL TECHNOLOGY CONFERENCE, Ottawa, Canada, May 31-June 3, 1970. The Institute shall not be responsible for opinions or statements advanced in papers it sponsors.

2/ Sign-X Laboratories Inc., Essex, Conn., U. S. A.

1. Introduction

This paper describes and evaluates plume rise during stable conditions. Previous research has been interested, primarily, in obtaining plume rise in a neutral or unstable environment so that the concentration of pollutants on the ground downwind of the stack could be determined. Under stable conditions, the plume from a tall stack will generally not reach the surface. It is, however, necessary to consider plume rise under stable conditions in order to answer the following important questions. Will the plume penetrate a stable layer? What will be the height of, and pollution concentration in, the plume at various distances downwind just prior to inversion break-up (fumigation)?

A method of calculating plume rise under stable conditions, based on data obtained from studies of the Keystone plant near Indiana, Penn., will be presented.

2. Data Acquisition

Under contract from the U.S. Public Health Service, Sign X Laboratories, Inc. undertook a study of the plume rise from a large power plant in western Pennsylvania during May and October, 1968. The Keystone Generating Station has a capacity of 1800 mw from two identical units; associated with each unit is one 800 ft. (244 m.) stack and two 300 ft. cooling towers. Only one unit was operating during the two field expeditions.

A Bell 47-G helicopter was instrumented so that continuous measurements of temperature, wet-bulb depression, pressure height, and sulfur dioxide could be recorded. The time constants of the first three parameters are less than 0.2 seconds; the time constant of the SO_2 unit is between 2 and 2.5 seconds. Also recorded was the output from a device that measured the change in space charge and which has virtually instantaneous response. Since the particles in the plume have a charge (positive), the device can provide good measurements of the plume boundaries.

The sensing probe was mounted on a strut of the helicopter, well forward of the downwash. The helicopter was flown at an airspeed of 55 to 60 mph during all traverses and soundings. Each flight lasted about 1 1/2 hours.

Temperature soundings were made upwind of the stack at the beginning and end of each flight. In addition, upwind temperatures at plume top height and stack top height were obtained at intervals throughout the flight.

Two basic types of traverses were flown in order to define the plume geometry and SO_2 concentration. One consisted of a series of horizontal traverses through, and normal to, the plume at a fixed distance downwind. These traverses were made at intervals of 30 meters from the top to the bottom of the plume.

The data obtained from one such series taken at 3.4 km downwind are shown in Figs. 1, 2 and 3. Examples of raw data gathered during three of this series of ten traverses are shown in Figs. 1a, b, c. The maximum SO_2

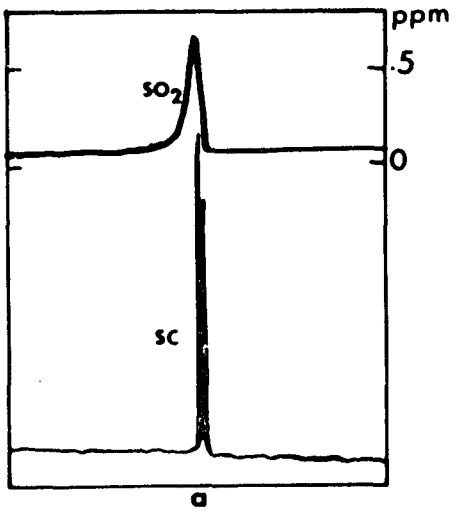

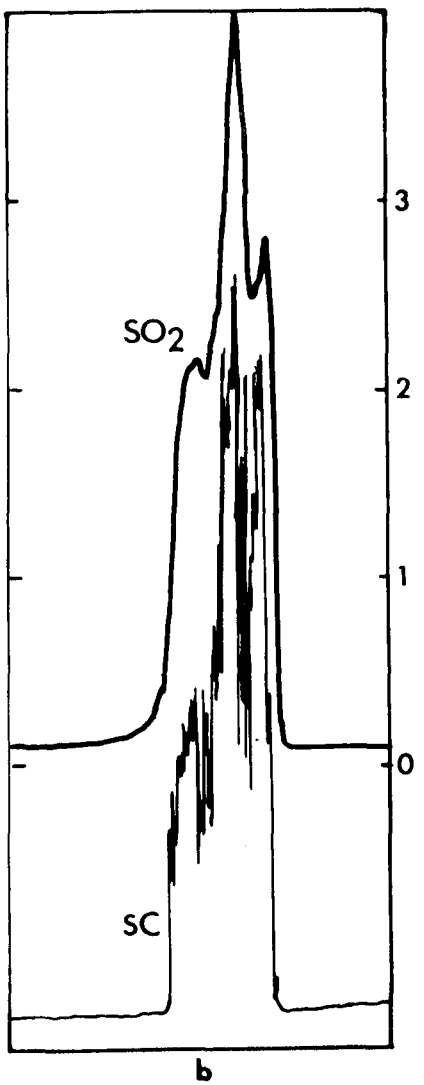

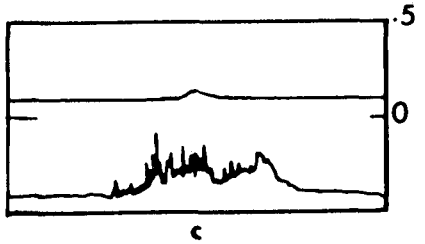

Fig. 1

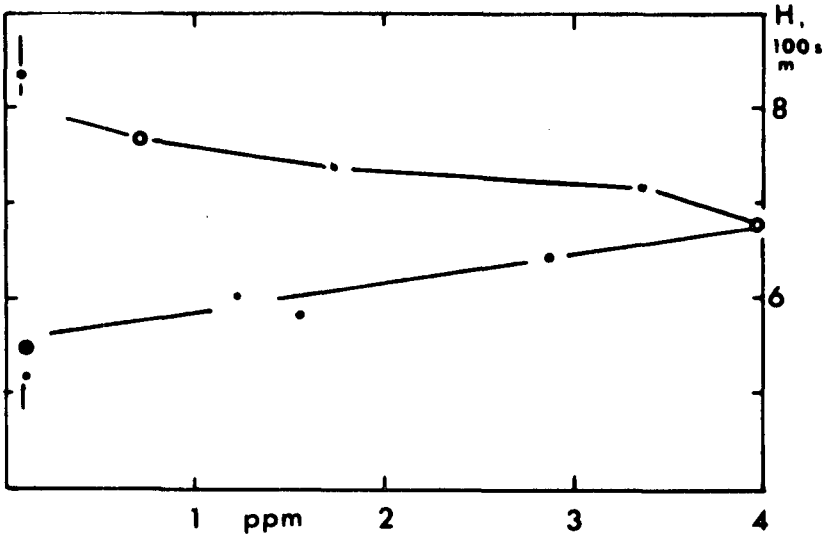

Fig. 2

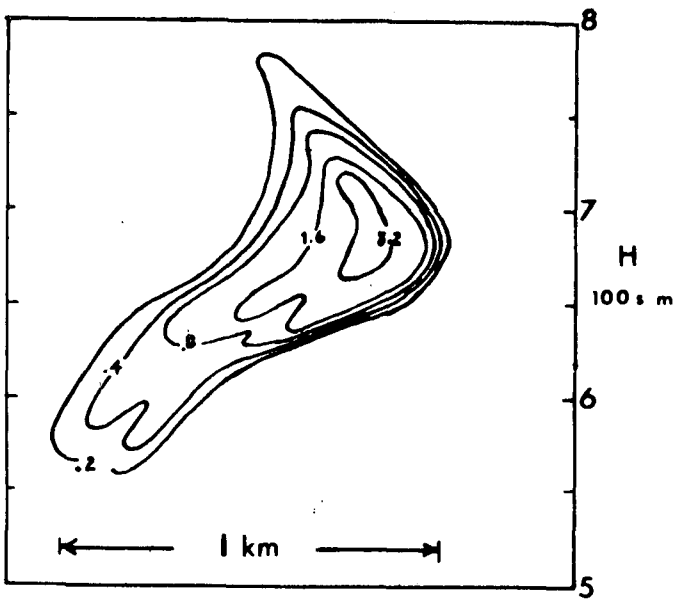

Fig. 3

Fig. 1a, b, c. SO_2 and space charge derivative during horizontal traverses through top, center, and bottom of plume respectively at a distance of 3.4 km downwind.

Fig. 2. The maximum SO_2 value as a function of altitude obtained on each traverse during ten horizontal traverses through the plume. (The circles at 775m, 680m and 550m are the max. values drawn in Fig. 1a, b, c.)

Fig. 3. Isolines of SO_2, drawn from SO_2 values obtained during the series of ten horizontal traverses.

values from these three traverses, plus those from the seven other traverses during the series, are plotted in Fig. 2. Fig. 3 shows isolines of SO_2, drawn from values obtained during the series. The viewer is looking down the plume. There was considerable directional wind shear at the time, which probably accounts for the plume tilt.

The second pattern consisted of a series of climbing and descending traverses through the plume from a distance of about 8 km. downwind. This pattern would take 5 or 6 minutes to complete, compared to 10-20 minutes for completion of a series of horizontal traverses.

Wind speeds and directions were obtained by PHS personnel every half hour using double theodolites. Interpolated values for every 50 meters were supplied. There was often early morning ground fog which prevented one or both theodolites from tracking the pibal. When this happened the average wind speed throughout the plume depth was obtained by determining the ground speed of the helicopter during a series of slanting traverses and subtracting the indicated airspeed. Comparision of these derived values with those obtained by double theodolite showed differences that were usually less than about 0.5 m/s.

The stack parameters (velocity and temperature of effluent) were supplied by PHS. The velocity was about 20 m/s and the temperature about 125°C above ambient. Stack diameter is 10.3 meters.

3. Definition of Terms

Plume rise is dependent upon the wind speed and atmospheric stability in the vertical region from stack top to plume top. This height difference is often measured in hundred of meters when large sources are considered (and we are concerned here only with comparatively large sources).

The wind speed at stack top level may differ from the mean wind in the vertical region from stack top to plume top by a factor of two or more. Therefore the mean speed, $\bar{u}$, has been used in all computations in this paper.

The plume may often penetrate a stable layer and enter a neutral layer aloft or it may rise through a neutral or slightly stable region to one of increased stability. In either situation the potential temperature gradient, $\partial\theta/\partial h$, at stack top level (or at any fixed height) is not representative of the atmospheric stability which determines plume height. In this paper the stability parameter includes the term $\Delta\theta/\Delta h$, where $\Delta\theta$ is the difference in potential temperature, and Δh the difference in height, between stack top and plume top. (See Fig. 4.)

Plume rise is generally defined as the height of the plume centerline above the stack top. This height, designated Δh_m in this paper, is defined as the height of the plume top above stack top, Δh, minus one half the plume thickness, Δz. ($\Delta h_m = \Delta h - \Delta z/2$)

The two heights, Δh and Δh_m, will generally change with increasing distance downwind. Under moderate or highly stable conditions the plume will rise and then may descend. It will have "overshot" its equilibrium level. Temperatures of up to 3°C below ambient have been measured in the upper portion of the plume in this "overshoot" region. At Keystone this region was 1 or 2 kilometers downwind; the equilibrium level was reached at 3 or 4 km and beyond this distance the plume height and thickness remained fairly constant.

Under neutral or slightly stable conditions the plume top height and plume thickness increase with increasing distance downwind. At Keystone, temperature excess was generally measured in the plume center about 2 km. downwind. At about 3 km. the difference was negligible.

Therefore, plume rise, for all cases from neutral to highly stable, was determined from plume boundaries measured at a distance of from 3 to 4 km. downwind.

4. Reduction of Data

Plume heights and potential temperatures were determined and plotted as a function of time for each flight day. An example is presented in Fig. 5. This diagram shows the potential temperatures at plume top level, θ_p, stack top, θ_s, and 20 meters above stack base, θ_g, all measured just upwind of the plant. It can be seen that there was a strong ground based inversion at the start of the first flight and that the second flight continued until inversion break-up. It should be noted that θ_g and θ_s are at fixed heights whereas the height of θ_p varies as the elevation of the plume top increased as a function of time.

From approximately 60 hours of such flight data, 20 cases have been selected for analysis. (See Table I.) The average wind speed varies from 4.8 to 12.5 m/sec. and the potential temperature lapse rate from 0.16 to 1.54 deg./100 m. Examples of fanning and lofting plumes are included. A classical coning plume was never seen, but one case may be classified as windy, near neutral. Looping plumes are, of course, not included because unstable cases are not considered in this analysis. There are, however, examples (e.g. the 1st case on 16 Oct.) which represent the situation during inversion break-up just prior to fumigation.

The duration of each case varies from about 5-10 minutes to 50 minutes. If wind speed, stability, and plume heights remained fairly constant for even as long as about 50 minutes (e.g. 1st flight on 16 Oct. - see Fig. 5), then this was counted as one case rather than five cases of 10 minutes duration.

There has been some smoothing of data, primarily measurements of plume base. The base was not as distinct and consistent as the plume top, which was usually readily identifiable.

The plume thickness, Δz, for each of the 20 cases is plotted in Fig. 6 as a function of stability.

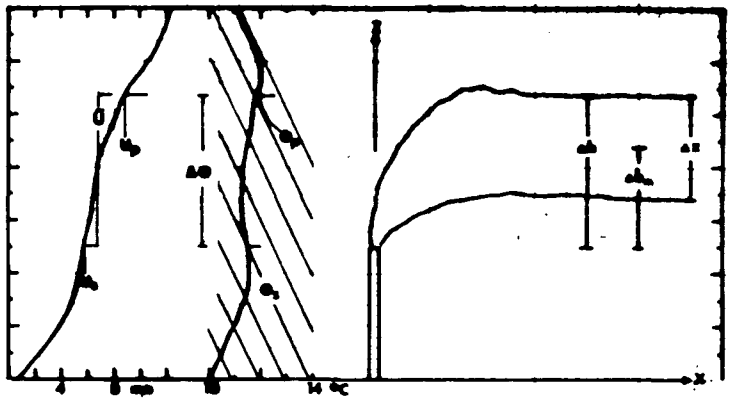

Fig. 4

Wind speed and temperature (left half of figure) are shown as a function of pressure height. The sloping lines are dry adiabats, i.e. each line represents a constant value of potential temperature. The outline of a typical plume, under stable conditions, is shown on the right. (Pressure height may be taken to be equivalent to actual height.)

NOMENCLATURE

- Δh - height of plume top above stack top (m)
- Δh_m - height of plume centerline above stack top (m)
- Z - height above stack base (m)
- H - pressure height (m)
- Δz - plume depth (m)
- θ_p - potential temperature at plume top (°K)
- θ_s - potential temperature at stack top (°K)
- θ_g - potential temperature at stack base plus 20m (°K)
- T_s - stack gas temperature (°K)
- T_a - ambient temperature at stack top (°K)
- $\partial\theta/\partial h$ - lapse rate between stack top and plume top
- $\Delta\theta/\Delta z$ - potential temperature gradient
- V_s - stack gas velocity (m/s)
- g - acceleration of gravity (m/s^2)
- $\bar{u}$ - mean wind speed between stack top and plume top (m/s)
- u_p - wind speed at plume top (m/s)
- u_s - wind speed at stack top (m/s)
- D - diameter of stack (m)
- G - stability parameter = $\frac{g}{T_a} \frac{\Delta\theta}{\Delta h}$
- F - buoyancy flux = $g V_s \left(\frac{D}{2}\right)^2 \left(\frac{T_s - T_a}{T_a}\right)$

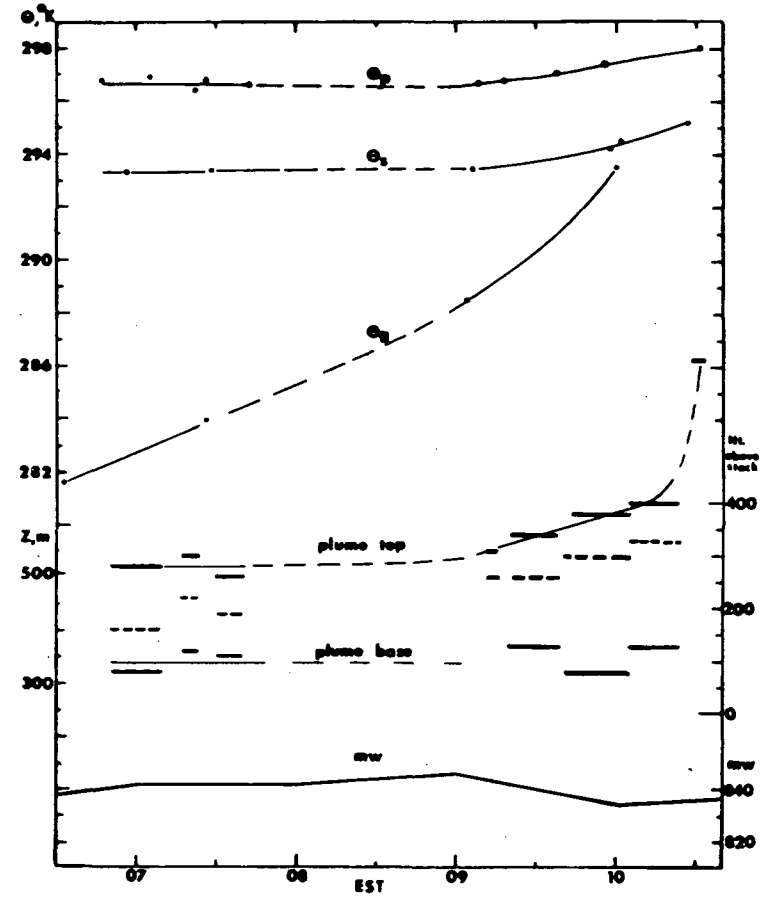

Fig. 5 16 Oct. 1968

Potential temperatures at plume top, θ_p, stack top, θ_s, and stack base level plus 20 m., θ_g, as a function of time. Heights of plume top and bottom, obtained from horizontal and slanting traverses, are shown as solid bars. The heights of max. SO_2 are shown as dashed bars. The plant output, in megawatts, is also presented. The first flight was from 0630 to 0745 EST and the second from 0900 to 1030.

Fig. 7 shows a plot of the maximum SO_2 concentrations obtained during slanting traverses for two days. One plot represents concentrations obtained during a 40 min. period on 20 Oct. when the average wind speed was about 8 m/s and stability about 1.5 deg./100m. The other plot represents data during a 40 min. period on Oct. 23 when the average wind speed was about 12 m/s and the stability 0.4 deg./100m. Further analysis of these, and other plots, should yield values of σ_y and σ_z for various wind and stability conditions.

5. Analysis of Results and Comparison with Various Formulae

The data for the 20 cases presented in Table I may be plotted in numerous ways. One plot is shown in Fig. 8, which shows the difference in potential temperature between stack top and plume top, $\Delta\theta$, as a function of stability. This is not a usual presentation; its value as an aid for predicting plume rise will be discussed subsequently. For the moment, it should be noted that at the higher stabilities (i.e. above about 0.8 deg./100m) the potential temperature difference remains fairly constant and is independent of wind speed. As the stability decreases, the effect of wind speed increases.

The height of the plume centerline, above stack top, Δh_m, for each of the 20 cases, is plotted in Fig. 9 as a function of stability. The two dashed lines represent the centerline height if the ASME formula (1) for stable conditions

$$\Delta h_m = 2(F/\bar{u}G)\cdot 33 \qquad [1]$$

is applied.

The two dotted lines represent the result from Holland's equation (2):

$$\Delta h_m = \frac{V_s\, d}{\bar{u}} \left(1.5 + 2.68 \times 10^{-3} p \, \frac{T_s - T_a}{T_a} \right) \qquad [2]$$

Values were chosen for the exit velocity, V_s, and temperature excess, $T_s - T_a$, of the effluent so that F, the buoyancy flux, would equal 2.2×10^3, the average value of the Keystone data. The atmospheric pressure, p, in [2] was chosen to be 984 mb., the approximate pressure at the Keystone stack top level.

Holland suggests that a value between 0.8 and 0.9 times the Δh_m obtained from the equation should be used for stable conditions. To obtain the slope for the two dotted lines in Fig. 9 values of 1.0, 0.9, and 0.8 times the Δh_m from [2] were applied when the stability equaled 0.1, 0.23 and 0.6 deg./100m respectively.

The same conclusion may be drawn from Fig. 9 as from Fig. 8; i.e. the plume rise at the higher stabilities is independent of wind speed but at lower stabilities the wind speed becomes increasingly important. The data fits the Holland formula best at low stabilities and fits the ASME best at higher stabilities. The former is often used to determine plume rise under neutral conditions because it is "conservative", i.e. it tends to underestimate. It should not, however, be applied to highly stable conditions, especially at low wind speeds.

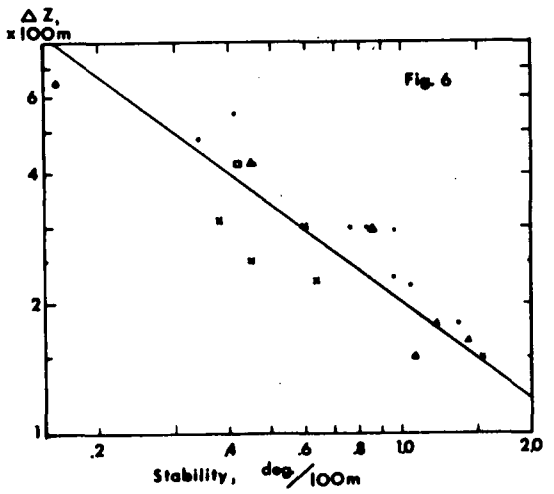

Fig. 6 (above). Plume thickness, Δz, as a function of stability.

o $\bar{u} < 6.0$ m/s
▲ 6.0 m/s < $\bar{u}$ < 8 m/s
x 8.0 m/s < $\bar{u}$ < 11 m/s
□ $\bar{u} > 11$ m/s

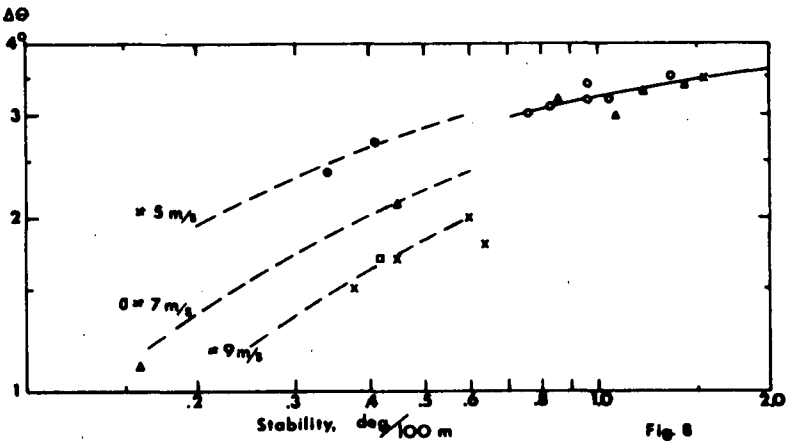

o $\bar{u} < 6.0$ m/s
Δ 6.0 m/s < $\bar{u}$ < 8 m/s
x 8.0 m/s < $\bar{u}$ < 11 m/s
□ $\bar{u} > 11$ m/s

Fig. 8 (above). The difference in potential temperature between stack top and plume top vs stability, for various (approximate) wind speeds.

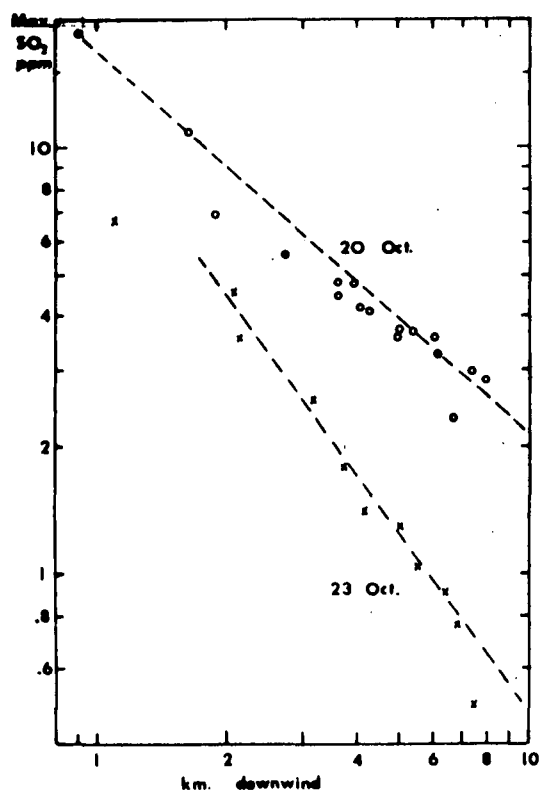

Fig. 7 Maximum values of SO_2 obtained during traverses on 20 Oct. (circles) and 23 Oct. (crosses) as a function of distance downwind of the stack.

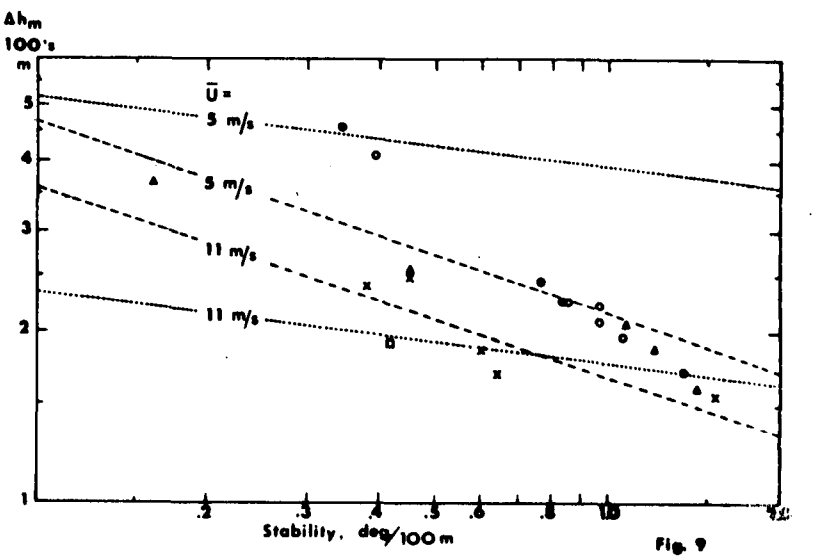

o $\bar{u} < 6.0$ m/s
Δ 6.0 m/s < $\bar{u}$ < 8 m/s
x 8.0 m/s < $\bar{u}$ < 11 m/s
□ $\bar{u} > 11$ m/s

Fig. 9 Observed plume rise, for Keystone data, as a function of stability. The two dashed lines represent the ASME formula for stable conditions; the two dotted lines represent Holland's formula.

(It should be noted that if plume rise is calculated from the ASME equation [1] using data from the Keystone studies, and compared to the measured plume rise, then 20% of the calculated values are within 10% of the measured values, when values for the wind speed and potential temperature gradient at stack top level are employed. If, however, $\bar{u}$ and $\Delta\theta/\Delta h$ are used instead, then 60% of the calculated values lie within 10% of the observed.)

Fig. 9 indicates that Δh_m for the Keystone data is proportional to about the -0.6 power of the stability and the zero power of $\bar{u}$ above about 0.8 deg./100m. As the stability decreases the data indicates that the magnitude of the stability exponent should decrease and that the magnitude of the wind speed exponent should increase.

If we assume that the plume rise from a comparatively tall stack, which emits an effluent at a velocity at least 1.5 or 2.0 x the wind speed at a temperature significantly above ambient, is dependent only on the stability, G, average wind speed, $\bar{u}$, and buoyancy flux, F, then we may write:

$$\Delta h_m \propto F^a \, G^{-b} \, \bar{u}^{-c}$$

When the stability is neutral, the exponent, b, will obviously equal zero, so that by applying simple dimensional analysis:

$$\Delta h_m = C \, (F \, \bar{u}^{-3})$$

This is similar to the ASME equation for neutral stability (ref. 1) where C = 150.

At high stabilities the data indicate that the exponent, c, equals zero, so that by applying simple dimensional analysis

$$\Delta h_m = C \, (F^{1/4} \, G^{-3/8}) \qquad [3]$$

For intermediate stabilities we may write, for example

$$\Delta h_m = C \, (F^{1/2} \, \bar{u}^{-1} \, G^{-1/4}) \qquad [4]$$

and a whole series of equations, of which eq. [1] is a member.

The observed plume centerline heights, Δh_m, are plotted in Figs. 10, 11, 12, applying [4], [1] and [3] respectively. The constant, C, is 4.5, 2.0 and 1.48 respectively.

We may "optimize" the fit in each figure by changing the constant, C, depending upon either the wind speed (primarily at low stabilities) or the stability (primarily at high stabilities). Or we may alter each equation by adding a constant. For example, in Fig. 12, if we write:

$$\Delta h_m = 2.36 \, (F^{1/4} \, G^{-3/8}) - 114 \qquad [5]$$

then all calculated values are within 10m. of the observed, at stabilities above 0.8 deg./100m. The writer would hesitate to claim this accuracy for the data.

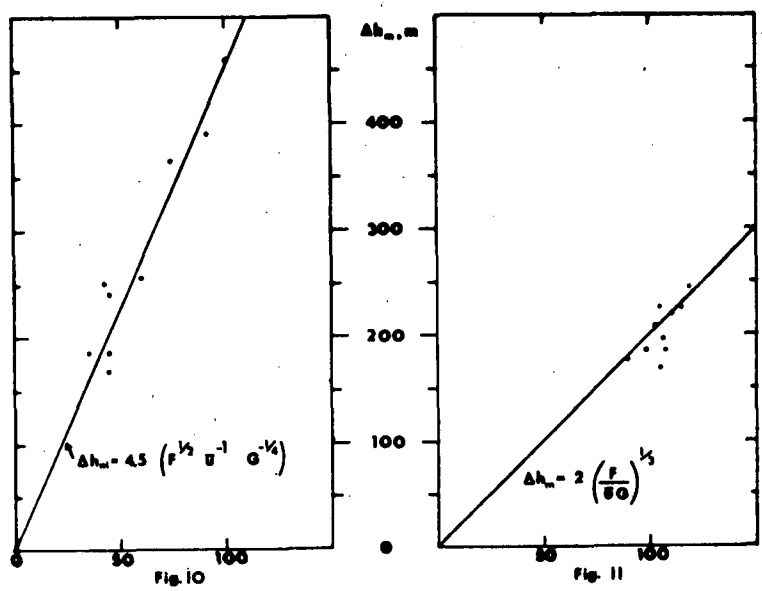

Fig. 10

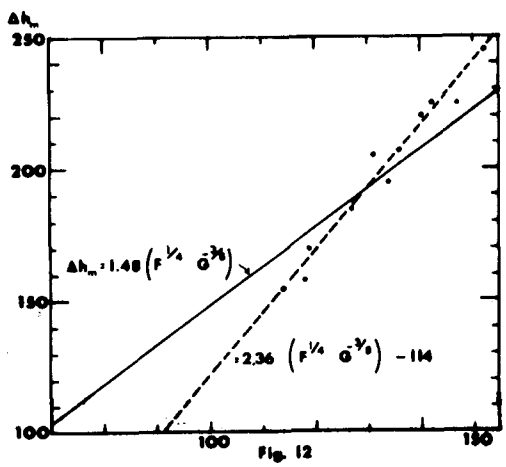

Fig. 12

Fig. 10
Plume rise vs. $F^{1/2}\ \bar{u}^{-1}\ G^{-1/4}$
Keystone data for stabilities between .16 and .64 deg./100m

Fig. 11
Plume rise vs. $(F/\bar{u}G)^{1/3}$
Keystone data for stabilities between .6 and 1.2 deg./100m

Fig. 12
Plume rise vs. $F^{1/4}\ G^{-3/8}$
Keystone data for stabilities between .76 and 1.54 deg./100m

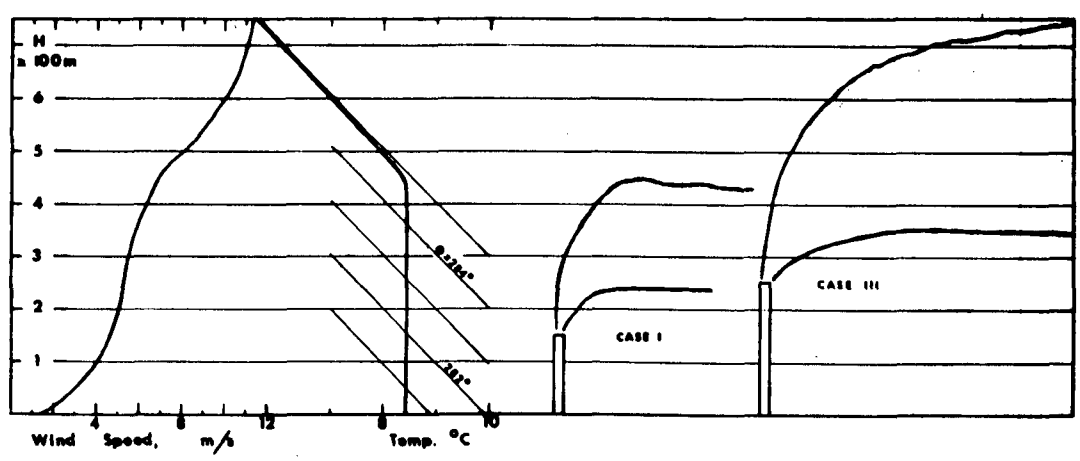

Figure 13

Wind speed and temperature are shown as a function of pressure height, H. Case I shows the probable plume outline from a 150 m. stack and the Case III shows the plume outline if the stack top were at 250 m.

This now becomes a mathematical exercise and it is better left to the mathematician. Suffice it to say that the exponents a, b and c, and the constant, C, are a function of both wind speed and stability.

The writer would prefer to use a series of diagrams, based on both the formulae and observed meteorological data, when plume rise is to be determined. This approach is described in the next section.

6. The Use of Diagrams

It has been strongly recommended that the mean wind speed, $\bar{u}$, and stability, $\Delta\theta/\Delta h$, between stack top and plume top be employed when calculating plume rise. However, actual values of $\bar{u}$ and $\Delta\theta/\Delta h$ cannot be obtained until the plume top height is known. Furthermore, it has been suggested that the appropriate equation, e.g. [1], [3], [4], is a function of the stability, $\Delta\theta/\Delta h$, and perhaps also $\bar{u}$. It would be a time consuming process to arrive at the calculated plume rise height, Δh_m, when there is a significant change in the wind speed and stability with height.

In Fig. 8 it has been shown, for the Keystone data at stabilities above about 0.8 deg./100m, that the potential temperature difference between stack top and plume top, $\Delta\theta$, is independent of wind speed. (It should be noted that under highly stable conditions the wind speed seldom exceeds about 8.0 m/s.) Furthermore, $\Delta\theta$ remains comparatively constant above about 0.8 deg./100m. It is roughly 3.2°K. Since stability is defined as $\Delta\theta/\Delta h$, a good first approximation for plume top height for stabilities above about 0.8 deg./100m may be easily obtained:

$$\Delta h \simeq 3.2/\text{stability}$$

Fig. 8 is applicable when the buoyancy flux, F, is approximately 2.2×10^3. It is based on the Keystone data where the range of F, for the points plotted, is from 1.98×10^3 to 2.7×10^3.

By applying [5] and utilizing Fig. 6 ($\Delta h = \Delta h_m + \Delta z/2$) we may obtain a diagram that gives $\Delta\theta$ as a function of the buoyancy flux for various stabilities. (See Fig. 14.)

Let us proceed with some examples.

6.1. Examples

We will determine the stack height and buoyancy flux required in order that the effluent from a proposed fossil fuel plant will penetrate a ground based stable layer. Assume that the proposed site is in a valley that lies roughly north and south. The valley walls may be only a few hundred meters high, but their height is such that there is generally down valley flow during the night and early morning hours. Measurements made at the proposed site show that the typical profiles of wind speed and temperature, during the autumn months, are similar to those drawn in Fig. 13. An isothermal layer extends to about 450m. Above this layer the lapse rate is neutral (adiabatic) and there is an increase in wind speed. Assume also that the wind direction above the stable layer is westerly (i.e. cross valley).

Case I

Let us determine the plume rise if the stack top were at 150 m and the exit velocity and temperature excess of the effluent were such that the buoyancy flux, F, equaled 1.6×10^3. When the temperature profile is isothermal, then the stability, $\Delta\theta/\Delta h$, is about 1.0 deg./100m.

The diagram Fig. 14, shows the difference in potential temperature between stack top and plume top, $\Delta\theta$, as a function of the buoyancy flux and stability. If $F = 1.6 \times 10^3$ then it can be seen that the potential temperature difference, $\Delta\theta$, is 2.82° when the stability, $\Delta\theta/\Delta h$, is 1.0 deg./100m. The height of the plume top above stack top, Δh, is obviously 282m (2.82° ÷ 1°/100m) which is 432 m. above the ground (150 + 282). The plume depth, Δz, is about 200 m. when the stability is 1.0 deg./100m. (see Fig. 6); therefore the height of the plume centerline above stack top, Δh_m, is 182 m. ($\Delta h_m = \Delta h - \Delta z/2$). The plume outline is shown in Fig. 13. It has not penetrated through the stable layer, it will probably run along the valley, the depth is comparatively shallow and, when fumigation occurs, the ground level concentrations may be unacceptably high.

Case II

To insure that the plume top enters the neutral layer and reaches above, say, 500 m, Δh must equal 350m., (500m - 150m). At 500m θ_p would equal 284.9° and at stack top level, $\theta_s = 282°$; therefore $\Delta\theta = 2.9$, $(\theta_p - \theta_s)$, and $\Delta\theta/\Delta h$ must be .83 deg./100m. Referring to Fig. 14 it can be seen that this point, (.83, 2.9), lies roughly at $F = 2.2 \times 10^3$. A buoyancy flux greater than this would insure that the plume top would reach 500m and enter the neutral layer.

Case III

Let us assume that the stack top were raised to, say, 250m. With a similar buoyancy flux, (2.2×10^3), the plume top would obviously penetrate into the neutral layer which has a potential temperature of 285°. The potential temperature difference will equal 2.0°, (θ_p = 285° and θ_s = 283°) and the average stability, $\Delta\theta/\Delta h$, will decrease (because of an increase in Δh). Fig. 14 cannot be used, because it is applicable only at moderately high stabilities (above about 0.8 deg./100m).

So far we have not been concerned about the wind speed, $\bar{u}$, because we have been dealing with moderately high stabilities. We turn now to Fig. 8, which is a plot of $\Delta\theta$ vs. stability, $\Delta\theta/\Delta h$, for various mean wind speeds and is applicable when the buoyancy flux is approximately 2.2×10^3.

If $\Delta\theta = 2.0°$ and $\bar{u} \approx 7$ m/s, then the stability, $\Delta\theta/\Delta h = 0.4$ deg./100 and $\Delta h = 500$m. If $\bar{u} \approx 8$ m/s then $\Delta\theta/\Delta h = 0.5$ and $\Delta h = 400$m. The mean wind speed, $\bar{u}$, between stack top, at 250m, and estimated plume top, at 650m or 750m. (250m + 400 or 500m) should now be determined from the wind profile in Fig. 13. If $\Delta h = 500$m, then $\bar{u} \approx 8.2$ m/s and if $\Delta h = 400$m, then $\bar{u} \approx 7.5$ m/s. To narrow the 100m range of estimated Δh, we refer again to Fig. 8 and find $\Delta\theta/\Delta h$ when $\bar{u} \approx 7.8$ m/s (and $\Delta\theta = 2.0°$). It is about .46 deg./100m; therefore $\Delta h \approx 440$m.

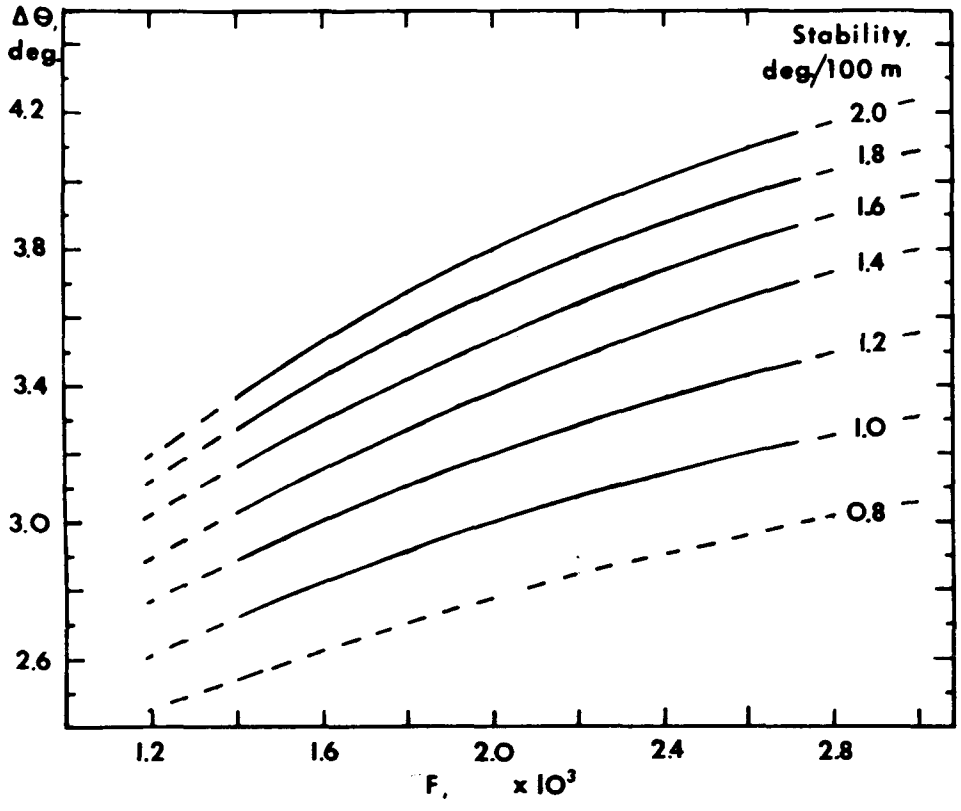

Fig. 14

The potential temperature difference, $\Delta\theta$, between stack top and plume top is shown as a function of the buoyancy flux, F, for various stabilities. The stability is defined as $\Delta\theta/\Delta h$, where Δh is the difference in height between stack top and plume top. Therefore, the height difference, Δh, equals $\Delta\theta \div$ stability. This diagram is based on the data shown in Fig. 12, which fits the equation,

$$\Delta h_m = 2.36\ (F^{1/4}\ G^{-3/8}) - 114$$

From Fig.6, the plume thickness, Δz, has been determined for the various stabilities and

$$\Delta h = \Delta h_m + \Delta z/2$$

Time EST	$\bar{u}$ m/s	$\Delta\theta$ deg.	$\Delta\theta/\Delta h$ $\times 10^{-2}$	$1/G$ $\times 10^{3}$	F $\times 10^{3}$	Δz m	Δh m	Δh_m m
16 Oct.								
0650-0740	6.0	3.3	1.20	2.47	2.21	180	275	185
0915	5.2	3.2	1.05	2.82	2.24	220	305	195
0930	5.2	3.2	.96	3.10	2.24	230	335	220
0955	5.4	3.1	.83	3.59	2.23	300	375	225
1010	5.2	3.0	.76	3.90	2.23	300	395	245
1030	4.8	2.7	.41	7.30	2.23	550	665	390
17 Oct.								
0645	8.5	1.8	.64	4.62	2.15	225	280	168
0715	8.8	2.0	.60	4.98	2.17	300	335	185
0915	7.0	2.1	.45	6.57	2.15	420	465	255
18 Oct.								
0650	9.8	1.7	.45	6.57	2.15	250	375	250
0725	9.5	1.5	.38	7.85	2.15	310	395	240
20 Oct.								
0650-0720	8.0	3.5	1.54	1.94	1.98	150	230	155
0905-0940	6.8	3.4	1.42	2.10	2.03	165	240	158
0955	5.8	3.5	1.35	2.20	1.99	180	260	170
1010	5.8	3.4	.96	3.11	1.99	295	355	207
1020	6.2	3.2	.85	3.51	1.99	300	375	225
23 Oct.								
0650-0740	12.5	1.7	.42	6.80	2.34	420	400	190
0910-0930	7.0	1.1	.16	18.10	2.70	650	690	365
24 Oct.								
0650-0730	4.9	2.4	.34	8.56	2.59	480	700	460
26 May								
0700	7.5	3.0	1.07	2.73	1.99	150	280	205

Table I

From Fig. 6, $z \simeq 360$m, so that $\Delta h_m \simeq 260$m., (440m - 360m/2). The suggested plume outline is drawn in Fig. 13. The exact value of Δh (or Δh_m) is not important. It will be about 440m (or 260m) at a distance of about 3 km. downwind and will continue to rise.

Thus, in our hypothetical example, we have determined that if the stack top height is 250m., and the buoyancy flux about 2.2×10^3, then the plume will rise above the stable layer into a region of increased wind speed where it will be carried across the valley. The plume depth will be comparatively great and when fumigation occurs, the ground level concentrations will probably be acceptable.

7. Conclusions

Plume rise is dependent upon the mean wind speed and average stability in the vertical region from stack top to plume top.

A single formula will not accurately predict plume rise for all ranges of stability and wind speed. A series of equations must be employed; the specific equation to be used is dependent upon the mean wind speed and average stability.

By introducing the concept of $\Delta\theta$, the maximum potential temperature difference that can be penetrated, the plume rise can be estimated comparatively easily and quickly with the aid of diagrams that are based on observed data and a series of equations.

8. Acknowledgements

The field studies at Indiana, Penn., and the subsequent reduction of data, were supported by the U.S. Public Health Service under contract no. PH 86-68-94. Further analysis and preparation of this paper were supported by Sign X Laboratories, Inc.

References

1. The American Society of Mechanical Engineers, May, 1968: Recommended Guide for the Prediction of the Dispersion of Airborne Effluents.

2. Holland, J.Z., 1953: A meteorological survey of the Oak Ridge area. 554-559 Atomic Energy Comm., Report ORO-99, Washington, D.C.